12-2013

Biochemical and Biophysical Studies of Novel Features of Ras-related Protein Interactions

Kyla Marie Morinini Morris
University of Arkansas, Fayetteville

Biochemical and Biophysical Studies of Novel Features of Ras-related Protein Interactions

Biochemical and Biophysical Studies of Novel Features of Ras-related Protein Interactions

A thesis submitted in partial fulfillment
of the requirements for the degree of
Master of Science in Chemistry

by

Kyla Morris
University of Arkansas
Bachelor of Science in Chemistry, 2011

December 2013
University of Arkansas

This thesis is approved for recommendation to the Graduate Council

_____
Dr. Paul Adams
Thesis Director

_____
Dr. Suresh Thallapuranam
Committee Member

_____
Dr. Roger Koeppe
Committee Member

ABSTRACT

The *Ras* superfamily of G-proteins are of great research interest for structure-function relationships among proteins as they act as molecular switches in the regulation of various biochemical reactions in the cell. They are regulated by protein-protein interactions targeted to the highly flexible switch regions. Mutations in G-proteins or their effectors may cause alterations in structure and/or function that can lead to overactivity.

The *Ras*-related protein Cell division cycle 42 (Cdc42) is important in regulating cell-signaling processes. The T35A mutation in Cdc42 leads to a decrease in flexibility of the Switch I region responsible for effector binding [3]. The kinetics of the intrinsic GTP hydrolysis reaction were compared for Cdc42 (WT and T35A) in the absence and presence of a peptide derivative of PAK21 activated kinase (PBD46). The mutation does not affect the intrinsic GTP hydrolysis rate of Cdc42, but binding with PBD46 is altered by the mutation; in the presence of PBD46, GTP hydrolysis is completely inhibited for Cdc42 WT while partial recovery of GTP hydrolysis for Cdc42 T35A was observed in the presence of PBD46. The data obtained lead us to propose two slowly interconverting conformational states of Cdc42 T35A, both able to hydrolyze GTP, but one that shows a weakened affinity for PBD46.

Ras homolog enriched in brain (Rheb) is a member of the *Ras* superfamily of proteins known to regulate cell growth and proliferation by signaling the mammalian target of rapamycin (mTOR) pathway. The Tuberous Sclerosis Complex 2 protein (TSC2) regulates Rheb by functioning as a GTPase activating protein (GAP). At present, very little is known about the molecular features of the Rheb-TSC2 protein interaction. We present biochemical and biophysical data on the interaction of Rheb with TSC2 WT, using a shorter, 218 amino acid GTPase derivative of TSC2 (TSC2-218), as well as with the mutant TSC2-218 K114A, to

characterize the TSC2-218 constructs and their GAP activity towards Rheb. A decrease in secondary structure as well as a loss of GAP activity is seen in the K114A mutant compared to WT.

ACKNOWLEDGEMENTS

I would like to start off by thanking my research group. Firstly, thank you to my research advisor, Dr. Paul Adams. When I joined the lab as an undergraduate student, I didn't know the first thing about research. I remember being told that I "think like a technician". At the time, I hated to hear that, but now I understand what he meant and I am proud to say that I no longer think like a technician (although I may still have my moments). Dr. Adams has helped me learn to think about things in more than one way and that there isn't always a right answer. To the fellow members of my research lab, thank you for being there with me through my course as a graduate student. Someone else was always in the lab at crazy hours, so we were able to keep each other company. I have found such reward in being able to turn around and teach you about the techniques that we use and why your experiments are important. I hope that I was able to influence your research experience in some way as you have influenced mine.

I need to thank the Department of Chemistry and Biochemistry for the opportunity to be a T.A. Through my T.A. assignments, I realized that teaching is what I truly love to do and, as a result realized that I want to spend my life teaching chemistry.

Also, a special thanks to my support system: my friends and my family. My friends, in particular Theresa Nguyen and Andrea Samuel, were always there to either listen to me complain about my struggles and to offer words of encouragement or to just be silly and make me laugh when I was too stressed and serious. A quote by Kurt Vonnegut comes to mind when I think of the times that I have gone to my friends: "Laughter and tears are both responses to frustration and exhaustion. I myself prefer to laugh". Surrounding myself with positive people made the whole process bearable. My family, although they don't usually make me laugh, support me in whatever it is that I want to do. Words of encouragement and just the comfort of their presence,

especially that of my mom, is sometimes the only thing that I need to make my day better and make me realize how proud I should be for what I accomplished.

Lastly, my husband, Andrew, deserves an award for putting up with the long hours spent in lab and the crazy schedule (or lack of schedule). They say that the first few years of marriage are the hardest to get through; I think that the first few years of a marriage while one person is working on a degree in chemistry are probably the hardest. He has always done whatever he could to help make things run more smoothly when I wasn't able to be around. I don't know how many times Andrew came to the lab late at night when I had something to work on (although he usually fell asleep while waiting on me to work). I know that if we made it through this stage together, we can make it through anything.

TABLE OF CONTENTS

TABLES

FIGURES

INDEX OF ABBREVIATIONS

BME	β-mercaptoethanol
CD	Circular dichroism
Cdc42	Cell division cycle 42
Cdc42 T35A	Cell division cycle 42 in which threonine at residue 35 has been mutated to alanine
Cdc42 (F28L)	Cell division cycle 42 in which phenylalanine at position 28 has been mutated to leucine
CV	Column volume
D_2O	Deuterium oxide
DSC	Differential Scanning Calorimetry
DNAse	Deoxyribonuclease I, from bovine pancreas
EDTA	Ethylenediaminetetraacetic acid
FPLC	Fast protein liquid chromatography
GAP	GTPase activating protein
GDI	Guanine dissociation inhibitor
GDP	Guanosine diphosphate
GEF	Guanine nucleotide exchange factor
GMPPNP	Guanosine 5'-[β,γ-imido] triphosphate; a non-hydrolysable GTP analog
GST	Glutathione-*S*-Transferase; affinity tag
GTP	Guanosine triphosphate
GTPase	GTP hydrolyzing protein
His_6	hexahistidine tag; affinity tag
HSQC	Heteronuclear single quantum correlation
IDT	Integrated DNA Technologies
IPTG	Isopropyl-β-d-thiogalactopyranoside
ITC	Isothermal titration calorimetry

LB	Lysogeny broth
mTOR	mammalian Target Of Rapamycin
NMR	Nuclear magnetic resonance
PAK	p-21 activated kinase
PBD46	46 amino acid derivative of PAK-21 binding domain
PBS	Phosphate buffered saline
PDB	Protein Databank
P_i	Inorganic phosphate
PMSF	Phenylmethanesulfonylfluoride
RBD	Ras binding domain
Rheb	*Ras* homolog enriched in brain
SDS	Sodium dodecyl sulfate
SDS-PAGE	Sodium dodecyl sulfate polyacrylamide gel electrophoresis
TBC1D7	Tre2-Bub2-Cdc16 1 domain family, member 7
TCA	Trichloroacetic acid
TSC1	Tuberous sclerosis complex 1
TSC2	Tuberous sclerosis complex 2
TSC2-218	218 amino acid binding domain construct of TSC2; corresponds to residues 1525-1742 of full-length TSC2
TSC2-218 K114A	218 amino acid binding domain construct of TSC2 with a lysine to alanine mutation at position 114 (position 1638 in full-length TSC2)
WT	Wild type

1 CHAPTER 1: INTRODUCTION

1.1 *RAS*

Structure-function relationships among proteins are crucial for evaluating the biological processes associated with these proteins. Understanding the chemical and biological aspects of these interactions can give much insight into how therapeutic treatments may be developed to combat diseased-states such as cancer. The *Ras* superfamily of G-proteins are of significant research interest as they act as molecular switches in the regulation of various biochemical reactions in the cell and are controlled via cycling between nucleotide-bound states[4]. Their cell signaling activity is dictated by the bound nucleotide; a biologically active GTP-bound form and an inactive GDP-bound form.

Ras proteins have been highly conserved through eukaryotic evolution [5]. Three *ras* genes have been identified in mammals, H-*ras*-1, K-*ras*-2, and N-*ras*, and are known as p21 [6-8]. All known *Ras* proteins contain 85 identical amino acids at the amino terminus. The subsequent 80 amino acids vary within the different proteins, although there is 85% homology between any pair of *Ras* proteins. The last domain exhibits the most variation among *Ras* proteins, although the carboxyl terminus always ends in C-A-A-X-COOH, where A is any aliphatic amino acid; this is important so that the protein can be targeted to the periphery of the cell membrane after it has been biosynthesized by lipidation [9].

Although comprised of multiple subfamilies with varying functions in the cell, *Ras* GTPases share similar structure in a G domain, the GTP/GDP binding domain [10]. This G domain includes the switch I, switch II and P loop regions (phosphoryl binding loop) [11]. Residues 25-40

make up the switch I region and residues 57-75 make up the switch II region responsible for hydrophobic, polar, and charged interactions with the effectors [12-15]. *Ras* contains a highly conserved glycine (G12) in the P-loop [11, 16]. The nucleotide binding region exhibited in *Ras* GTP-binding proteins is highly conserved [17]. The phosphate groups of the nucleotide interact at the P loop, with a general sequence ^{10}GXXXXG^{15}, as well as residues 116-119 with a sequence ^{116}NKXD^{119} [18, 19]. Mutation of the glycine at position 12 to anything other than proline leads to inherent activation [20-22], which can also occur if this residue is deleted or if insertions occur immediately before [23]. Changes in this residue disrupt the α-helical structure lead to improper folding [24-26]. If the subsequent glycine (G13) is mutated to either valine or aspartic acid, oncogenic activity is induced in the protein [27]. *Ras* also contains a conserved glutamine residue (Q61) in the nucleotide binding domain that stabilizes the nucleotide and is, therefore, important for GTP hydrolysis [28-30]. This residue is the most frequently mutated residue in human cancers; replacement of leucine for this glycine increases the GTP bound levels by causing resistance to *Ras* GAP activity [31]. The cycling between the GTP- and GDP-bound states of *Ras* GTPases is a result of the high affinity of the G domain for these nucleotides [32] and is catalyzed by regulatory proteins (**Figure 1**). The GTP-GDP exchange is stimulated by guanine nucleotide exchange factors (GEFs), which interact at the switch I and switch II regions**.** Upon binding to GTP, a conformational change is induced in *Ras* that favors protein-effector interactions that facilitate activity [33]. GTPase-activating proteins (GAPs) stimulate GTP hydrolysis; hydrolysis causes a

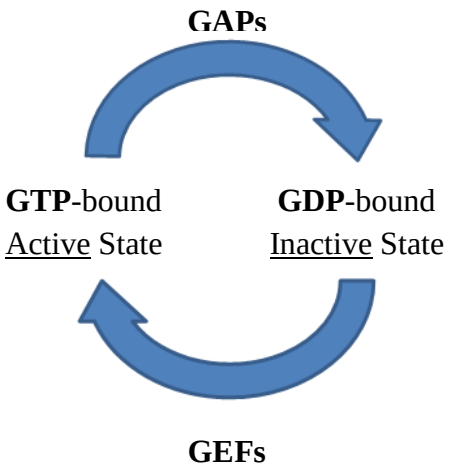

Figure 1. G-protein GTP/GDP cycle. GAPs and GEFs regulate the active and inactive states.

conformational change that lowers the protein's affinity for effectors, thereby causing inactivation. *Ras* GAPs work to stabilize the conserved switch II glutamine responsible for stabilization of the hydrolytic water responsible for hydrolysis of the γ-phosphate through the use of an arginine residue that forms hydrogen bonds with a bridge oxygen atom of GTP [31, 34, 35]. Guanine dissociation inhibitors (GDIs) stabilize the GDP-bound form of GTPases and prevent membrane localization [36]. Abnormal expression, often as a result of various mutations, in GTPases is responsible for a large proportion of cancer types. Mutations often lead to a loss of GTPase activity which prolongs the GTP-bound conformation and keeps the GTPase in an uninterrupted active state; extended overactivity often results in cancer [9, 37]. Abnormal expression in *Ras* proteins have been implicated in up to 30% of human cancers [37]. For these reasons, the GTPases are hopeful drug targets for anticancer therapy.

1.2 Cdc42

Cdc42 is a member of the rho subfamily of the *Ras* superfamily of GTPases, which plays significant roles in the regulation of cell proliferation and differentiation by binding to effectors; upon effector binding, a cascade of kinase interactions is activated. P21-activated kinase, a serine/threonine kinase, is one such kinase [38]. Like other *Ras* proteins, Cdc42 has the potential to signal overactivity if its active state is not regulated as GTP concentration in the cell is much higher than that for GDP [38]. A 46-amino acid peptide derived from PAK (PBD46) interacts with Cdc42 with high affinity [38, 39] and prevents GTP hydrolysis by stabilizing Cdc42 in the GTP-bound state with a slow exchange rate [38]. This interaction, which occurs in the highly flexible switch I and switch II regions [33, 38], initiates a signaling cascade leading to the activation of multiple kinases [40]. PBD46 was derived from PAK1, one of the four subtypes of PAK, and NMR structures have revealed that, while unstructured in its free form, PBD46 undergoes a

conformational change upon binding to Cdc42 [41]. This conformational change is partnered with a decrease in flexibility exhibited in Cdc42 upon interaction [38].

Structural studies on Cdc42 have identified 6 β-sheets, 5 α-helices and 10 loop regions [42]. NMR solution studies have shown that PBD46 interacts primarily with a β-strand (β2) via an antiparallel intermolecular extension, as well as with portions of α1, α5, switch I, and switch II [38, 39, 41]. Further NMR studies by Gizachew, et al. implied that the Cdc42-PBD46 interaction is stabilized by hydrophobic interactions and that the strong binding energy can be attributed to the interaction between the carboxylate group of glutamic acid at position 15 in PBD46 and the hydroxyl group of tyrosine at position 40 in Cdc42.

The switch I and switch II regions are both highly flexible regions responsible for effector interaction. Single point mutations involving various residues in the Switch I region have an effect on the effector binding of *Ras* proteins [43]. The phenylalanine at position 28 is important as its aromatic ring stabilizes the nucleotide [82-84]. Mutation of phenylalanine to leucine at this position in Cdc42 (Cdc42 F28L) is referred to as a fast cycling mutant; it is characterized by an increased exchange rate between GTP and GDP [85]. This rapid exchange can be attributed to an increase in flexibility in the nucleotide binding site that lowers the affinity for the nucleotide [85]; specifically, NMR studies indicated that the F28L mutation altered the binding site around the α and β phosphate groups of the nucleotide, but no modifications were seen around the γ phosphate [17, 86]. Also in the Switch I region of Cdc42, as with other *Ras* proteins, an invariant threonine at position 35 is critical for function. Preliminary observation of a threonine to alanine point mutation at this residue (Cdc42 T35A) shows that, although the thermal stability is not effected, less effector binding occurs and this weakened interaction may be a result of the

loss of conformational freedom in the Switch I region, supported by solution structure backbone dynamics studies and biochemical characterization, due to the removal of the hydroxyl side chain of residue 35 [3, 44]. Our hypothesis is that the weakened binding between Cdc42 T35A and PBD46 could restore the GTP hydrolysis activity characteristic of Cdc42. We use a GTP hydrolysis assay to compare the intrinsic GTP hydrolytic activity of Cdc42 T35A to Cdc42 WT in the absence and presence of PBD46. The results show that both Cdc42 T35A and Cdc42 WT, in the absence of PBD46, demonstrate similar hydrolytic efficiency. However, Cdc42 T35A still exhibits a fraction of GTP hydrolysis in the presence of PBD46 in contrast to the complete inhibition observed for WT. The data suggest that there may be multiple slowly interconverting conformations of Cdc42 T35A that may have different or weakened interactions with PBD46. This study highlights the potential for development of a way to restrict flexibility as a means to control oncogenic protein-protein interactions.

1.3 RHEB

Rheb (*Ras* homology enriched in brain) proteins belong to the *Ras* superfamily of G-proteins [21, 45]. Due to the cycling between GDP and GTP, as with other *Ras* proteins, Rheb must be regulated through protein-protein interactions. Upon binding to GTP, a conformational change from the GDP-bound form is induced, which allows Rheb to regulate cell growth through its role in signaling through the insulin/TOR/S6K pathway [46-50]. Overall sequence similarity is seen between Rheb and *Ras*, with a few key differences [49]. Rheb contains an arginine (R15) at the position equivalent to the conserved glycine (G12) in *Ras* [20-22]. Substitution of glycine for arginine at position 15 in Rheb does not restore hydrolytic activity as would be expected for its equivalence in *Ras*[51]. In Rheb, mutation of the homologous glutamine residue to leucine (Q64L) does not inhibit protein-protein interactions; this residue is catalytically useless, due to its buried

orientation in a hydrophobic pocket, and does not participate in GTP hydrolysis [1, 45, 52]. Due to these differences, Rheb has an intrinsically low rate of GTP hydrolysis and, as such, must be regulated by protein-protein interactions in order to prevent overactivity by remaining in the GTP-bound active state [20, 53, 54]. Therefore, outlining the correlation between structure and function is crucial for understanding, at the molecular level, what underlies the onset of the diseased-state.

The genes of the tuberous sclerosis complex, TSC1 and TSC2, were first identified as tumor suppressor genes [55]. The TSC1 gene encodes for the protein TSC1 (hamartin), which has a "coiled-coil" domain near its carboxy terminus; this domain binds with high specificity to a domain found at the amino terminus of TSC2 (tuberin) [54, 56]. TSC1 and TSC2 interact to form a heterodimer called the tuberous sclerosis complex (TSC). The TSC1 and TSC2 proteins share limited homology with any other proteins [57] with the exception of the C-terminus of TSC2 which contains a highly conserved domain that is homologous to Rap1GAP [55, 58]. It was suggested that the GAP domain of TSC2 interacts directly with a GTPase in order to facilitate the tumor-suppressing function of the complex [54, 55, 59]. Rheb was determined to be a direct target for TSC GAP activity [45-47, 52, 55, 60]. The TSC1/TSC2 complex functions as a Rheb GAP; an interaction between Rheb and TSC2 mediates the mTOR pathway and therefore regulates cell growth and energy and nutrient levels (**Figure 2**). An extensive search of the literature does not reveal the specific role of TSC1 in the Rheb/TSC2 interaction [46, 50, 53, 55, 61, 62], only that it is required for the stabilization of TSC2 against ubiquitination [63, 64]. As a GAP, TSC2 stimulates GTP hydrolysis in Rheb through what has been suggested to be a catalytic "asparagine thumb" based on the homology to Rap1GAP, which also functions via the "asparagine thumb" [65-67]. TSC2 differs from its interaction in Rheb from other *Ras* GTPases and their GAPs in the presence of this

"asparagine thumb" as mentioned. This interaction differs in that it is not characterized by the "arginine finger" motif present in the activation of other GTPases like *Ras* [34]. Incorporation of an arginine residue in place of the asparagine residue that resulted in complete loss of GAP function proved that TSC2 could not function via a *Ras*GAP-like "arginine finger" mechanism [45]. Therefore, it is necessary to outline the molecular features of the Rheb-TSC2 protein-protein interaction that are important in the regulation of cell-signaling pathways dictated by this interaction.

A truncated version of TSC2 containing the GAP domain (TSC2-218) has been shown to interact with Rheb *in vitro* [45]. Mutations in the GAP domain of TSC2 have been described as leading to the onset of tuberous sclerosis, a genetic disorder associated with benign tumors called hamartomas that are often accompanied by the onset of seizures and mental retardation, due to the function of the GAP domain to increase intrinsic Rheb GTP hydrolysis activity; when mutated, the GAP activity of TSC2 towards Rheb is altered [46, 53-55, 68-70] (**Figure 3B**). The underlying biological mechanism by which TSC2 catalyzes GTP hydrolysis is not yet completely understood, but examination of disease-associated GAP domain mutants of TSC2 can allow for the study of the molecular mechanism of TSC2 GAP activity. Our hypothesis is that mutations in TSC2 are either unable to bind to Rheb, and therefore unable to function as GAPs, or they bind, but are unable to catalyze GTP hydrolysis.

Through the use of several biochemical and biophysical techniques including circular dichroism and differential scanning calorimetry, it is apparent that the K114A mutation in TSC2-218 leads to a change in secondary structure and thermal stability; these structural differences, compared to WT, could explain the loss GAP activity towards Rheb seen in the kinetics studies and the lack of binding seen in the binding assays. Where TSC2-218 WT functions to stimulate

Rheb GTP hydrolysis, a very low rate, similar to that of Rheb, was seen for Rheb in the presence of TSC2-218 K114A, suggesting that either TSC2-218 K114A does not bind to Rheb at all or that it binds with no catalytic activity towards Rheb. This study emphasizes the need to characterize the Rheb-TSC2-218 complex in order to get a detailed molecular picture of TSC2's catalytic mechanism as there is minimal information on the Rheb-TSC2 interaction due to the lack of structural information on TSC2-218.

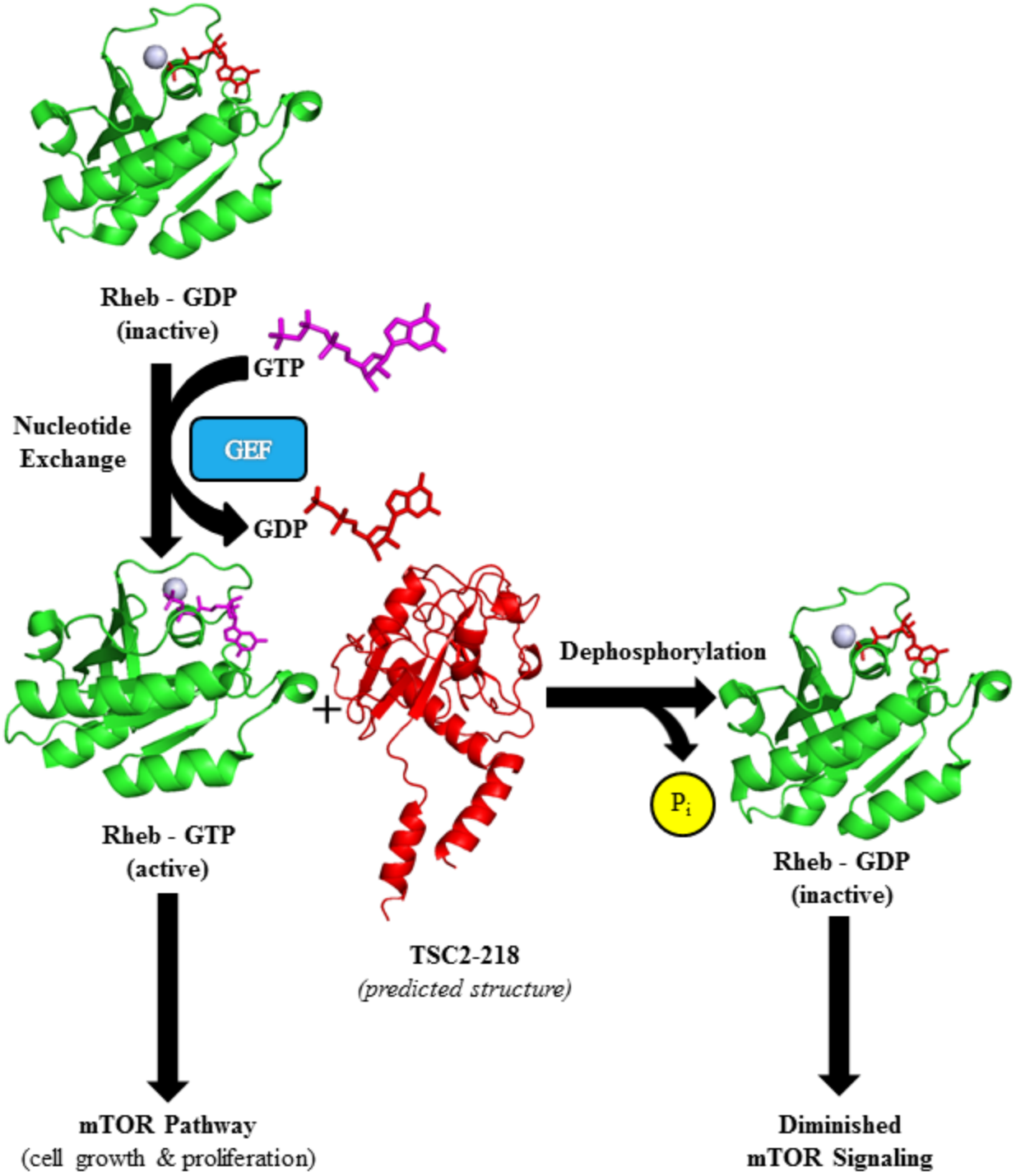

Figure 2. Schematic illustration of the TSC2-stimulated GTPase activity of Rheb. The activity of Rheb is controlled by the nucleotide-bound state; GTP-bound Rheb (1XTS.pdb) is active and GDP-bound Rheb (1XTQ.pdb) is inactive. The binding of TSC2 to active Rheb-GTP (1XTS.pdb) [1] stimulates hydrolysis which diminishes the mTOR activity. The structure of TSC2-218, currently unknown, was predicted using I-TASSER [2].

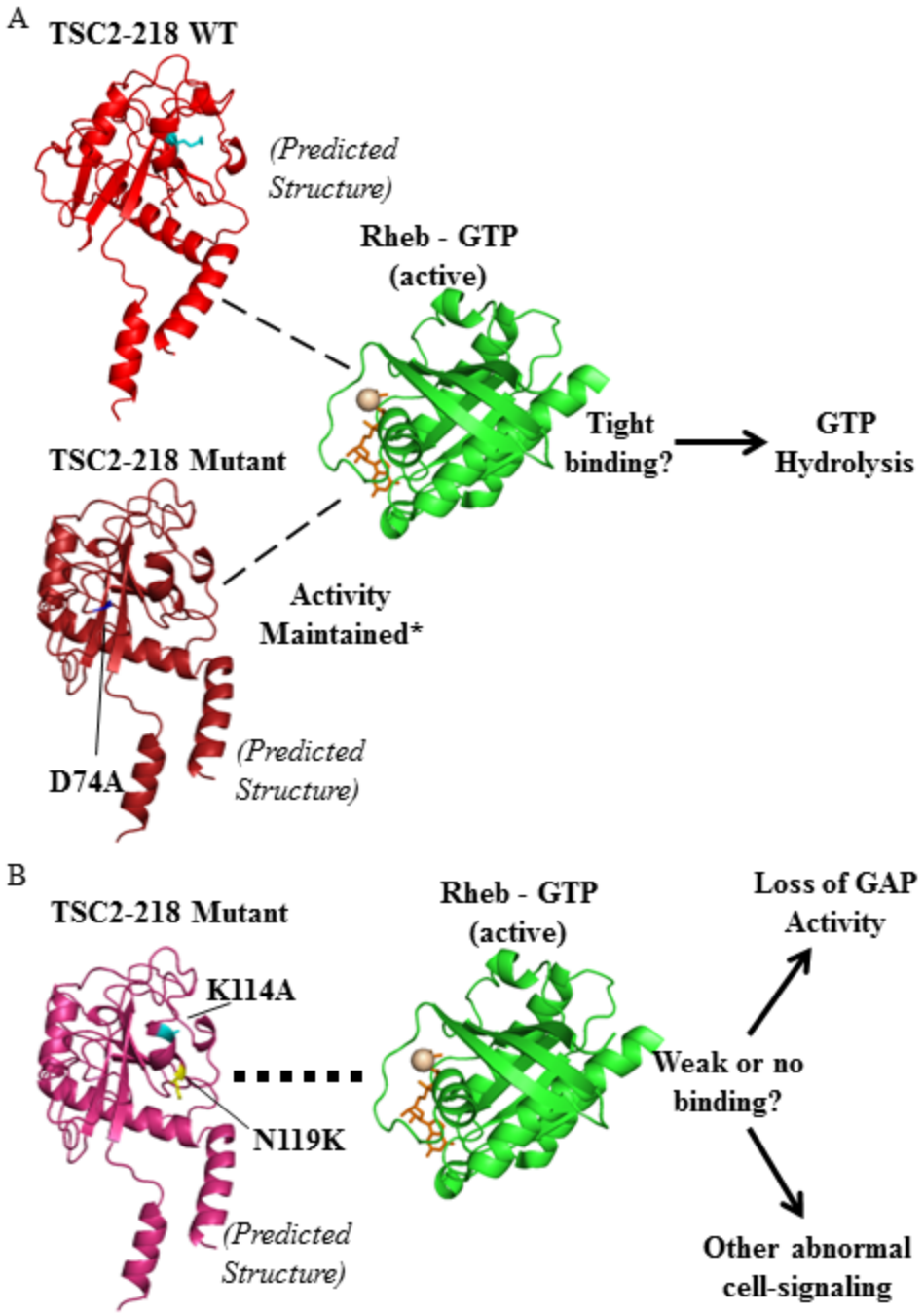

Figure 3. Regulation, or lack thereof, of TSC2-stimulated GTPase activity of Rheb. (A) TSC2-218 WT functions as a GAP for Rheb by facilitating GTP hydrolysis and inhibiting over-activity, represented by the longer dashed lines indicating a stronger interaction. (B) Mutant TSC2-218 shows weaker or no binding to Rheb (shorter dashed lines) leading to abnormal cell-signaling activity or a loss of GAP activity. The structure of TSC2-218, currently unknown, was predicted using I-TASSER [2].

2 CHAPTER 2: EXPERIMENTAL

2.1 PROTEIN GROWTH, EXPRESSION AND PURIFICATION

2.1.1 CDC42 (WT AND T35A)

Cdc42 constructs were overexpressed as His_6-tagged fusion protein from pET15b in the *Escherichia coli* strain BL21 (DE3) in LB broth. A culture of LB containing 0.1 mg/mL ampicillin was grown overnight at 37°C. This overnight culture was used to inoculate 1-2 liters of fresh LB and was allowed to grow with shaking at 37°C until the OD_{600} reached 0.6-0.8. The cells were induced with a final concentration of 0.2 mM IPTG (isopropyl-β-D-thioglactopyranoside) and allowed to express at 37°C for 4 hours. After expression, the cells were harvested by centrifugation at 6,500 rpm for 20 minutes at 4°C. The pellet was resuspended in 10 mM Tris (pH 8.0) and centrifuged again. The cell pellets were stored at -80°C.

To begin the purification process, each 1-liter pellet was thawed on ice and resuspended in lysis buffer (25 mL Tris/NaCl binding (40 mM imidazole, 100 mM NaCl, 50 mM Tris pH 8.0, 10 mM $MgCl_2$), 25 mg lysozyme, Halt protease inhibitor cocktail to a final concentration of 0.5x, DNAse, and 1 mM PMSF). Cells were lysed via sonication on ice (3 second pulse with 5 second pause, 40 repetitions). The cell debris and the soluble fraction were separated by centrifugation at 18,000 rpm for 25 minutes at 4°C. The cell lysate as well as Tris/NaCl binding buffer and Tris/NaCl elution buffer (250 mM imidazole, 100 mM NaCl, 50 mM Tris pH 8.0, 10 mM $MgCl_2$) were filtered before purification on AKTA FPLC using a 5-mL prepacked Ni^{2+} affinity column (GE Healthcare HiTrap His Column). After the column was equilibrated with 5CV Tris/NaCl binding buffer, the cell lysate was loaded over the column. A linear gradient was used to increase the imidazole concentration for elution of the purified protein. The protein was either

dialyzed overnight at 4°C against the required buffer for the next experiment or lyophilized for storage. For active Cdc42, Cdc42-His_6 was nucleotide exchanged according to established procedures [71]. Briefly, Cdc42-His_6 was incubated with 5 mM EDTA and 0.5 mM GTP analog for 3 hours at 4°C. Following incubation, EDTA and excess nucleotide were removed with an equilibrated desalting column (GE Healthcare PD-10). 10 mM Mg^{2+} was replaced.

2.1.2 PBD46

PBD46, a peptide derivative of p21-activated kinase, was expressed as a GST fusion protein from pGEX-2T in the *E. coli* strain BL21 (DE3) in LB broth to OD_{600} 0.8-1.0 and induction with 0.5 mM IPTG for 5 hours at 37°C. GST-PBD46 was lysed as previously described for Cdc42, except that the binding buffer was PBS (137 mM NaCl, 2.7 mM KCl, 10 mM Na_2HPO_4, 2 mM KH_2PO_4, pH 7.4) [72]. A GSTrap FF 5 mL prepacked column (GE Healthcare) eluted with an isocratic gradient of glutathione elution buffer (10 mM reduced glutathione, 20 mM Tris pH 8.0) was used in purification.

As the GST tag is quite large (26 kDa), it was necessary to cleave off the tag. Thrombin recognizes a specific amino acid sequence between PBD46 and the GST tag. PBD46 was cleaved from the GST tag by incubation with thrombin (Sigma) for 5 hours at 4°C. After incubation, Halt protease inhibitor was added to stop cleavage. The product was dialyzed in PBS (pH 7.4) before loading onto a regenerated GST column as before to remove the GST tag.

2.1.3 RHEB

Residues 1-169 of Rheb were overexpressed as a His_6-tagged fusion protein as described for Cdc42 (page 11) using PBS Ni^{2+} binding (PBS pH 8.0, 50 mM $MgCl_2$, and 25 mM imidazole) and PBS Ni^{2+} elution (PBS pH 8.0, 50 mM $MgCl_2$, and 400 mM imidazole) buffers.

For active Rheb, Rheb-His_6 was nucleotide exchanged for one hour at room temperature.

2.1.4 TSC2-218 WT

As successful growth and overexpression of the GAP domain of TSC2 (TSC2-218) as a GST fusion protein from pGEX-2T in the *E. coli* strain BL21 (DE3) in LB broth had not yet been achieved in the lab, it was necessary to optimize these conditions. Existing stocks were used to streak agar plates containing ampicillin and allowed to grow overnight at 37°C. Isolated colonies were used to inoculate LB containing ampicillin. After expression (**Figure 4**), 1 mL samples of each were pelleted by centrifugation. The supernatant was discarded and the pellet

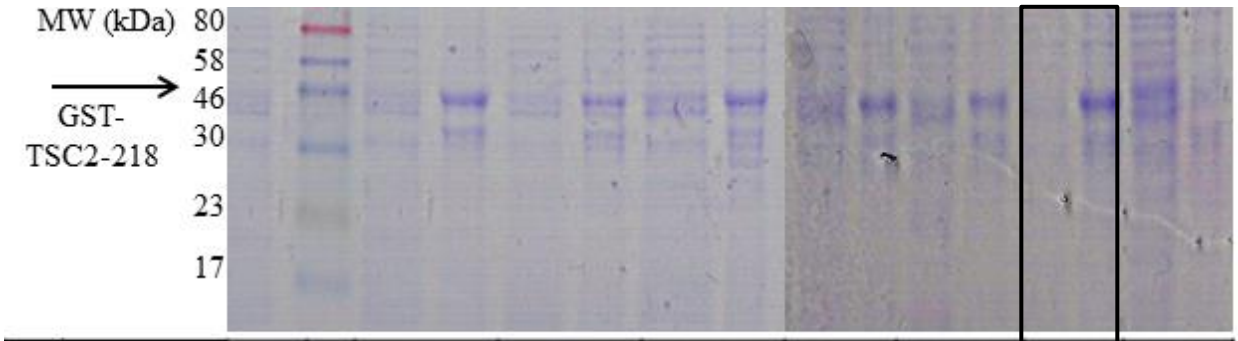

			Molecular Weight Marker	D		E		F		A		B		C		G	
	Sample	PI		D		E		F		A		B		C		G	
	OD_{600}	0.6		0.6		0.6		0.6		0.9		0.9		0.9		0.9	
	[IPTG] (mM)			1.0		1.0		0.5		1.0		1.0		0.5		0.5	
Expression	Temp (°C)			37		25		25		37		25		25		37	
Expression	Time (hr)			3		3		5-6		3		3		5-6		5-6	
Fraction	Soluble				X		X		X		X		X		X		X
Fraction	Insoluble			X		X		X		X		X		X		X	

Figure 4. GST-TSC2-218 Test Expression. After inoculated with overnight culture, samples were expressed according to conditions in table. Pre-induced sample (PI) taken at OD600 0.6. Condition C (OD600 0.8-1.0, 0.5 mM IPTG, room temperature expression for 5-6 hours) yields the highest expression of GST-TSC2-218 in the soluble fraction (demarked by black box).

was then resuspended in 100 μL lysis buffer (PBS (pH 7.4), 10 mM $MgCl_2$, and 0.1 mg/mL lysozyme). The soluble and insoluble fractions were then separated; the suspension was sonicated briefly and exposed to a freeze-thaw method of lysis. Centrifugation separated the soluble (supernatant) and insoluble (pellet) fractions. The pellet was resuspended in 8M urea. 2X sample dye (100 mM Tris (pH 6.8), 4% SDS, 20% glycerol, 200 mM BME, and 0.2% bromophenol blue) [72] was added to each sample before running on 15% SDS-PAGE. The density of each band corresponding to the molecular weight of GST-tagged TSC2-218 (51 kDa) represented a direct correlation to the amount of expression. Growth to OD_{600} 0.8-1.0 and induction with 0.5 mM IPTG at room temperature for 5-7 hours gave the highest yield of protein in the soluble fraction.

GST-TSC2-218 was lysed as previously described for GST-PBD46. To determine the necessary time required for cleavage, thrombin was added to the protein sample (1 unit thrombin per 150 μg protein) and incubated at 4°C. After each hour, a sample was removed and Halt protease inhibitor added to stop cleavage. After 4 hours, each sample was run on SDS-PAGE (**Figure 5**). TSC2-218 was cleaved from the GST tag by incubation with thrombin for 1-2 hours at 4°C as described (page 12).

2.1.5 TSC2-218 K114A

Using Qiagen Plasmid Prep Kit, a plasmid of TSC2-218 was prepared from a 5-mL overnight culture. The DNA concentration was determined via UV Vis at 260 nm. Once obtained, the DNA was submitted with pGEX 3' primer and pGEX 5' primer to University of Arkansas DNA Resource Center for sequencing. When the sequence of TSC2-218 WT was confirmed, primers were designed to make the lysine to alanine point mutation at position 114. When designing the primers for product TSC2-218 K114A, it was important that the primer sequence had minimal

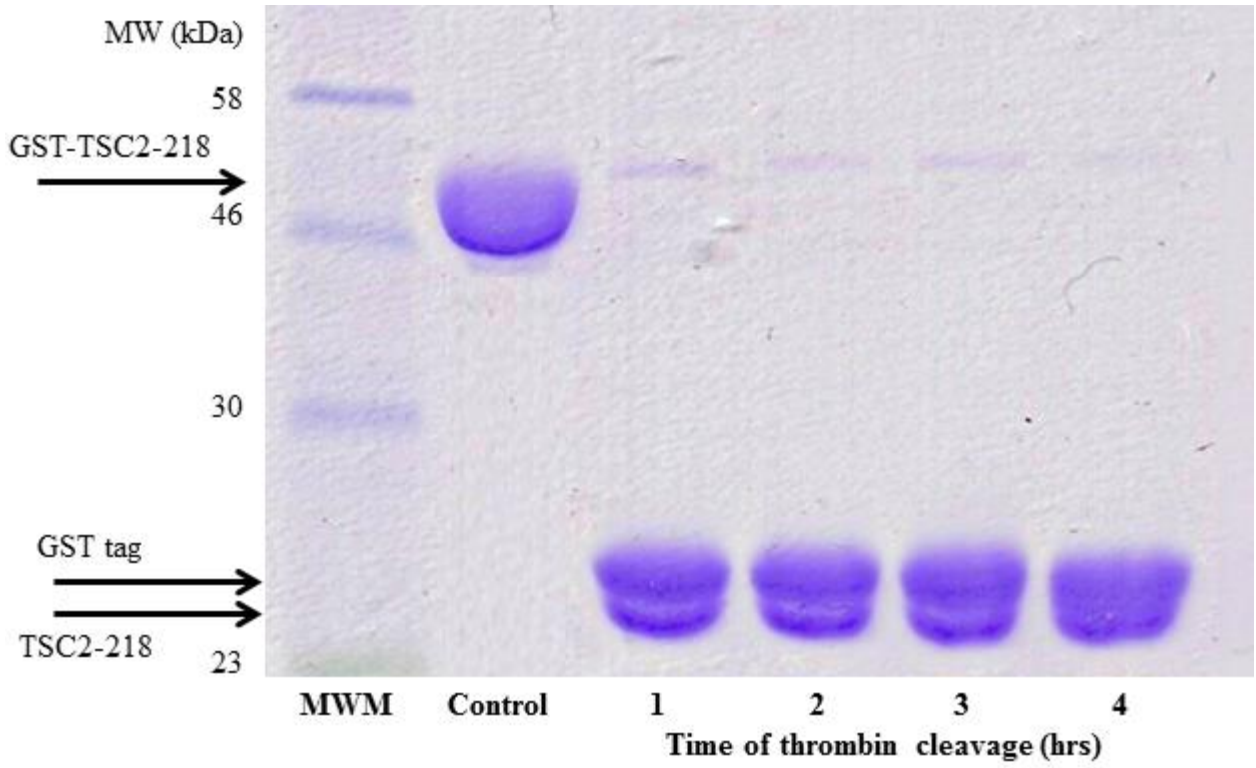

Figure 5. SDS-PAGE of thrombin cleavage experiment. Lane 1 shows the molecular weight marker. Lane 2 shows the GST-tagged TSC2-218 control. Lanes 3-6 show the thrombin cleavage products after 1-4 hours, consecutively. Thrombin cleavage is complete after 1 hour.

secondary structure, would not form a primer dimer, and that it had an acceptable G-C content reflected by the melting point. The codon AAG translates to lysine and alanine is coded by GCT, GCC, GCA, and GCG. The mutation of AAG to GCG was chosen as it requires the fewest nucleotide changes. OligoAnalyzer (IDT) was used to monitor the various combinations of primers for the optimal sequence. The forward and reverse primers used were:

Forward: CGACAAGGCGCGCCACCTGGG **Reverse:** CCCAGGTGGCGCGCCTTGTCG

DNA calculator (Sigma) was used to analyze the primers for T_m, GC content, secondary structure, and the likelihood of primer dimer formation; both primers show weak secondary structure, no primer dimer, and have a T_m of 81.21 °C.

A Quick Change Site Directed Mutagenesis Kit II (Stratagene) was used to form the point mutation. The sample was prepped according to the kit; 5 µL 10X reaction buffer, 5-50 ng dsDNA, 125 ng primer 1 (forward primer), 125 ng primer 2 (reverse primer), and1 µL dNTP mix were combined and made to 50 µL with sterile water followed by the addition of 1 µL DNA polymerase. The parameters on the PCR cycler are shown in **Table 1**. The amplified PCR product was digested by addition of DpnI restriction enzyme and 1 hour incubation at 37°C. A transformation into BL21 (DE3) competent cells immediately followed. This new construct was labeled TSC2-218 K114A.

Segment	Cycle	Temperature (°C)	Time
1	1	95°C	30 seconds
2	18	95°C	30 seconds
		55°C	1 minute
		68°C	2 min + ($^{1\ min}/_{kilobase\ DNA}$)
Set to hold at 4°C			

Table 1. PCR settings for site-directed mutagenesis. The kilobases of DNA for the protein and the primer totaled 5.638 kb. The time for the 68°C cycle of segment 2 was set at 7.638 minutes.

Plasmid prep was again prepared and DNA submitted for sequencing. Sequencing results showed that the point mutation was successful.

A test expression was repeated as described before (see page 13) to determine growth and expression conditions for GST-TSC2-218 K114A as the mutation may have altered expression in comparison to TSC2-218 WT. GST-TSC2-218 K114A was expressed at room temperature for 5

hours after induction with 0.5 mM IPTG. Purification was identical to that for GST-TSC2-218 WT.

2.2 *IN VITRO* BINDING ASSAYS

Rheb-His_6 was nucleotide exchanged according to previous protocols [71] (page 12) using GMPPCP (Sigma). Equimolar Rheb-His_6-GMPPCP and GST-TSC2-218 were incubated together at 4°C for 12-16 hours. The sample was concentrated to 1 mL and purified using size-exclusion chromatography. A HiPrep 16/60 Sephacryl S-100 HR column (GE Healthcare) was used on AKTA FPLC. 10 microliters of each concentrated fraction was run on a 15% SDS-PAGE. The *in vitro* binding assays were performed in triplicate.

2.3 CIRCULAR DICHROISM

Circular dichroism measurements were performed on a Jasco J-710 Spectropolarimeter. CD spectra of purified protein samples were measured in the far-UV range (190-250 nm) in a 0.2 mm pathlength quartz spectrophotometer cell. Spectra were measured at 50 nm/min. The concentration of protein solutions used for the CD measurements was 0.5 mg/mL in 10mM phosphate buffer (pH 7.0). For difference spectra, the protein and ligand protein were combined in a 1:1 ratio. Spectra Manager was used to collect the data in triplicate. 10 spectra were obtained for each sample. From each spectrum, the spectrum of the buffer was subtracted using Spectra Manager. For the difference spectra, the spectrum of the ligand protein was subtracted.

2.4 DIFFERENTIAL SCANNING CALORIMETRY

Differential scanning calorimetry measurements were performed using an N-DSC III Differential Scanning Calorimeter (Calorimetry Sciences Corporation). Purified protein concentrations of 1-2 mg/mL were dialyzed extensively at 4°C in 10 mM phosphate buffer at pH 7.4. Spectra of the

protein were recorded over a temperature range between 10 and 100°C at a heating rate of 2°C/min after degassing of the sample. A baseline obtained using the buffer was subtracted from the protein spectra. Each protein sample was scanned in triplicate. CpCalc (Calorimetry Sciences Corp) was used to obtain the melting curve and determine the T_m.

2.5 PROTEOLYTIC DIGESTION

Chymotrypsin (Sigma-Aldrich) and sodium dodecyl sulfate (J.T. Baker) were of molecular biology or ultrapure grade. Limited proteolytic digestion experiments on TSC2-218 were carried out at 25°C in 10 mM HEPES pH 8.0 in the presence of 10 mM $CaCl_2$. Proteolytic digestions were performed in triplicate at an enzyme (chymotrypsin) to substrate (TSC2-218) molar ratio of 1:15. The protease activity was stopped after desired time intervals by the addition 1% SDS and the pH adjusted to 2.0 by the addition of 1 μL 12.1 M hydrochloric acid (EMD) and heating for 5 minutes at 100°C to abolish all enzyme activity [73, 74]. The degree of proteolytic cleavage was measured from the intensity of the 24 kDa band on a 15% SDS−PAGE gel corresponding to the untreated protein (TSC2-218) using UN-SCAN-IT gel 6.1 software. The intensity of the protease-untreated 24 kDa band (TSC2-218) was used as the control for 100% protection against proteolytic digestion. Chymotrypsin control concentration was verified by UV-absorbance at 280 nm.

2.6 GTP HYDROLYSIS ASSAY

GTP hydrolysis assays were carried out to characterize differences of hydrolytic activity of WT vs mutant proteins for the Cdc42-PBD46 and Rheb-TSC2-218 interactions.

All chemicals were ultrapure or of molecular biology grade and all chemical solutions were prepared fresh before each assay. The *Ras* protein (Rheb or Cdc42) was nucleotide exchanged

using GTP by incubating the protein with freshly prepared 0.5 mM GTP (Sigma) and 5 mM EDTA (EMD) to remove bound Mg^{2+}. EDTA and any excess nucleotide were removed by passing through a PD-10 desalting column (GE Healthcare) and then 10 mM $MgCl_2$ was added to the protein solution to incorporate Mg^{2+} back on the protein. The *Ras* protein bound to GTP was immediately passed over a PD-10 column again to remove any endogenously hydrolyzed P_i released prior to the GTP hydrolysis assay.

Time-dependent GTP hydrolysis was performed with TSC2-218 using a 1:2.5 molar ratio of GTP-bound Rheb (10 μM) to TSC2-218 (25 μM). To initiate hydrolysis, each protein mixture was mixed with 2 mM GTP in 10 mM HEPES pH 8.0 (J.T. Baker) to a final volume of 1 mL and incubated at 25°C. For measuring GTP hydrolysis as a function of time, the hydrolysis was stopped after desired time intervals (0, 10, 20, 30, 45, 60, and 90 min) via protein denaturation by the addition of 6% SDS (J.T. Baker). For the GTP hydrolysis assay as a function of TSC2-218 concentration, 10 μM Rheb was incubated with TSC2-218 at varying concentrations for 30 minutes, and the hydrolysis measured at each concentration of TSC2-218. To monitor GTP hydrolysis, 6% ascorbic acid and 1% ammonium molybdate (Sigma) were added to the protein mixture, followed by 3-7 minute incubation at room temperature. Sodium citrate (Sigma), sodium metaarsenite (J.T. Baker), and acetic acid (EMD) (1% each) were added to the denatured protein mixture and incubated for an additional 20 minutes and then assayed for any color changes at 850 nm according to established methods (**Figure 6**) [75, 76]. To calibrate the assay, GTP was added after protein denaturation and the absorbance of this sample was read and subtracted from the desired sample absorbance at each time point. Using K_2HPO_4 as a phosphate source, 0-75 nM phosphate was assayed in triplicate to generate a linear standard curve used to calculate the amount of P_i released. The average change in P_i released as a function of time was

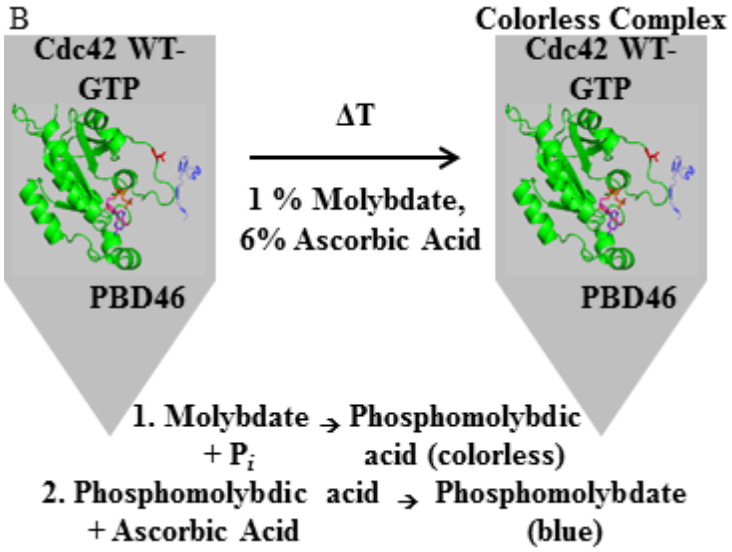

Figure 6. P_i monitoring by molybdate. (A) Cdc42 (WT), as well as Cdc42 (T35A), hydrolyzes GTP, evident by formation of the blue colored complex. (B) The interaction of PBD46 inactivates Cdc42 (WT) by preventing hydrolysis; no colored complex forms as no inorganic phosphate is released. Although molybdate and ascorbic acid were added, without phosphate present as a result of hydrolysis, no colored complex forms. (C) The weaker interaction of PBD46 with Cdc42 (T35A) partially restores hydrolysis. The lower yield of inorganic phosphate results in less colored complex formation, evident in the lighter blue color.

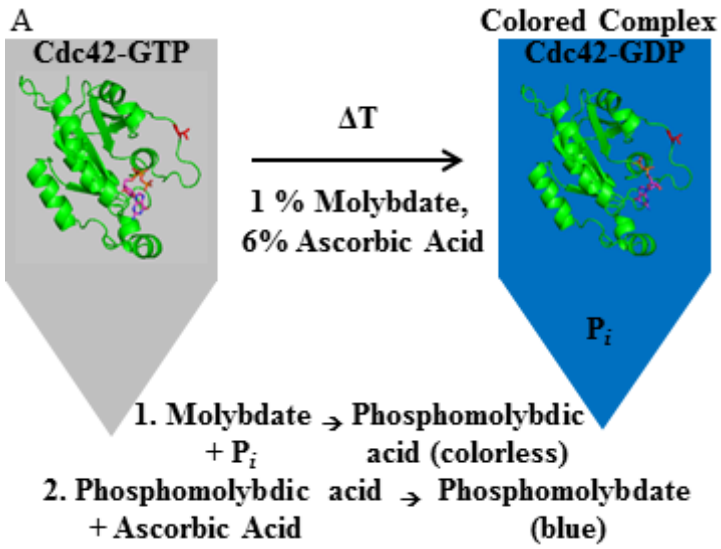
A
Cdc42-GTP
ΔT
1 % Molybdate,
6% Ascorbic Acid
Colored Complex
Cdc42-GDP
P_i
1. Molybdate + P_i → Phosphomolybdic acid (colorless)
2. Phosphomolybdic acid + Ascorbic Acid → Phosphomolybdate (blue)

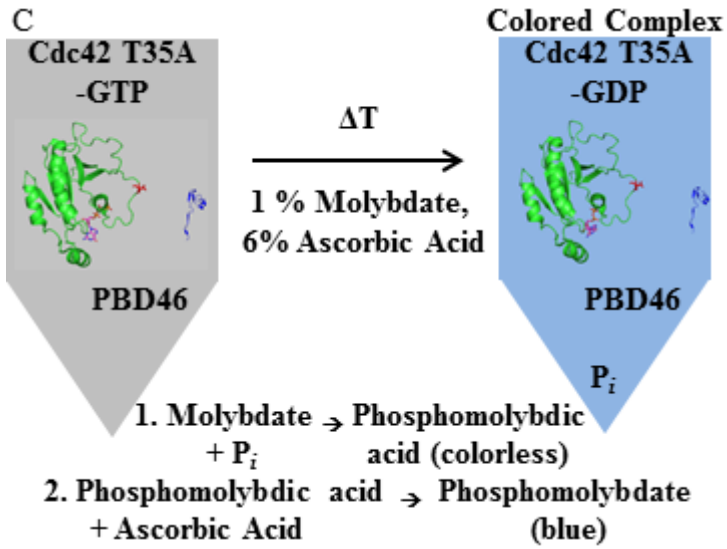
C
Cdc42 T35A
-GTP
PBD46
ΔT
1 % Molybdate,
6% Ascorbic Acid
Colored Complex
Cdc42 T35A
-GDP
PBD46
P_i
1. Molybdate + P_i → Phosphomolybdic acid (colorless)
2. Phosphomolybdic acid + Ascorbic Acid → Phosphomolybdate (blue)

determined by averaging the values from triplicate experiments and calculating the difference for each time point from the time-zero value. To measure GTP hydrolysis of Cdc42 (WT and T35A), the Cdc42 was assayed in the absence and presence of PBD46 as a function of time and as a function of PBD46 concentration as described for the Rheb-TSC2-218 interaction.

2.7 2D-HSQC NMR

2.7.1 Sample Preparation

To initiate growth, an overnight culture of either Rheb or TSC2-218 was grown in LB. The cells were pelleted via centrifugation and washed twice with NMR buffer (10 mM NaH_2PO_4, 5 mM $MgCl_2$, and 100 mM NaCl). The cells were resuspended in unlabeled M9 minimal media (47.8 mM Na_2HPO_4, 22 mM KH_2PO_4, 8.6 mM NaCl, 18.7 mM NH_4Cl, 2 mM $MgSO_4$, 0.1 mM $CaCl_2$, and 0.4% glucose supplemented with a vitamin solution (.325 mg each of pantothenoic acid, choline chloride, folic acid, myo-inositol, nicotinamide, pyridoxyal hydrochloride, and riboflavin) and 25 mg/L thiamine) [72] and allowed to grow overnight. The overnight culture was used to inoculate fresh M9 media and monitored for the highest expression yield. ^{15}N Rheb and ^{15}N TSC2-218 were overexpressed in $^{15}NH_4Cl$ enriched minimal medium according to the demarcation in **Figures 7 and 8**, respectively, by induction with IPTG at room temperature. Purification was the same as for unlabeled samples (pages 12-14).

2.7.2 Spectra Acquisition

2D NMR experiments were performed on a Bruker Avance-500 MHz or 700 MHz NMR spectrometer at 25°C using TopSpin NMR. 500 μL of 0.1-0.5 mM labeled was dialyzed (Tube-O-DIALYZER from G Biosciences) in NMR buffer (10 mM NaH_2PO_4, 5 mM $MgCl_2$, 100 mM NaCl, pH 5.5) and 15% D_2O was added. The spectra were processed using XWINNMR and Sparky software.

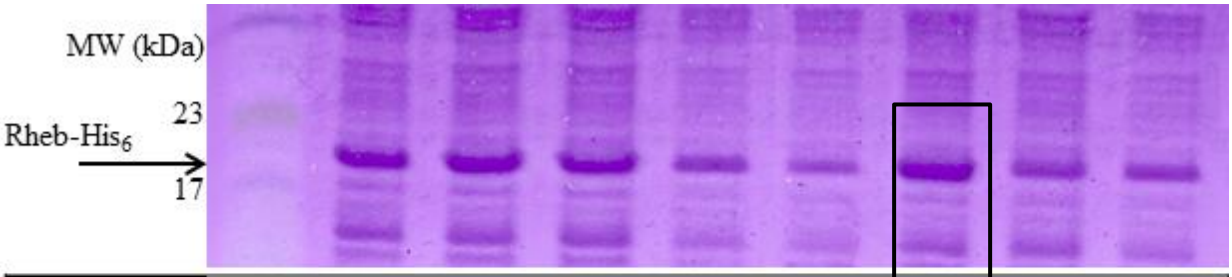

Lane	Molecular Weight Marker	A	B	C	D	E	F	G	H
OD_{600}		0.7	0.7	0.7	0.4	0.4	0.4	0.7	0.4
[IPTG] (mM)		0.2	0.2	1.0	0.2	0.2	1.0	1.0	1.0
Expression Temp (°C)		37	25	25	37	25	25	37	37

Figure 7. ^{15}N Rheb Test Expression. ^{15}N-Rheb Test Expression. Samples were expressed according to conditions in table. All samples expressed for 16 hours. Condition F (OD600 0.4, 1.0 mM IPTG, room temperature expression) yields the highest expression of ^{15}N-Rheb (demarked by black outline).

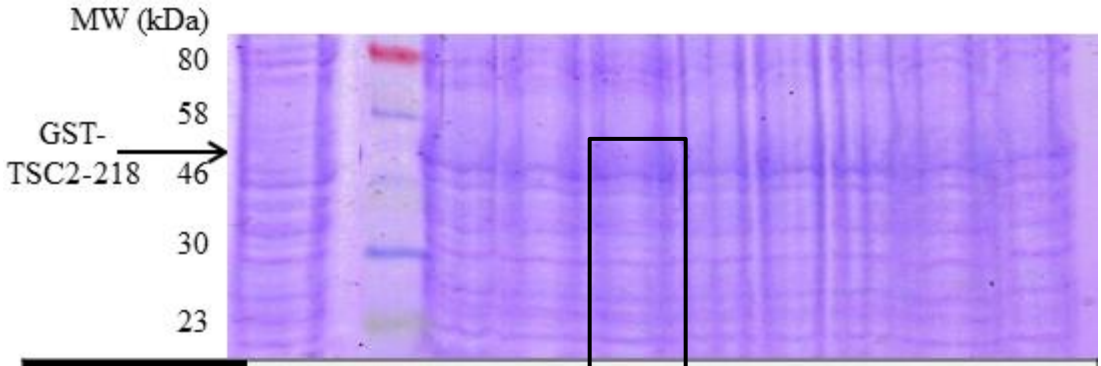

Lane	PI	Molecular Weight Marker	A	B	C	D	E	F	G	H
OD_{600}	0.4		0.9	0.9	0.7	0.7	0.9	0.9	0.7	0.7
[IPTG] (mM)			0.5	0.1	0.5	0.1	0.5	0.1	0.5	0.1
Expression Temp (°C)			25	25	25	25	37	37	37	37

Figure 8. ^{15}N-GST-TSC2-218 WT Test Expression. Samples were expressed according to conditions in table. All samples expressed for 16 hours. Condition C (OD_{600} 0.7, 0.5 mM IPTG, room temperature expression) yields the highest expression of ^{15}N-GST-TSC2-218 WT (demarked by black outline).

3 Chapter 3: Results and Discussion

3.1 Intrinsic GTP Hydrolysis is observed for a Switch I Mutant of Cdc42 in the Presence of a Specific GTPase Inhibitor Peptide Derivative

Studies on the conformational flexibility of a Cdc42 mutant show that with decreased flexibility, Cdc42 T35A binds to effector proteins less [3]. As previously described, PBD46 prevents GTP hydrolysis of Cdc42 [38]. To compare the effects of the hydrolysis of Cdc42 T35A to Cdc42 WT, we examined the GTP hydrolysis of Cdc42 (WT and T35A) both alone and in the presence of PBD46. Shown in **Figure 9**, a linear decrease in P_i released was seen for both Cdc42 WT and T35A, although variation is seen in the slopes. At a concentration of 10 μM PBD46, where the [Cdc42 WT]:[PBD46] = 1:1, total inhibition of GTP hydrolysis is seen. The saturation point for Cdc42 T35A was seen at approximately 16 μM PBD46, 1:1.6 [Cdc42 T35A]: [PBD46]. Further addition of PDB46 does not have an effect on the GTP hydrolysis of activity of Cdc42 T35A above this saturation point.

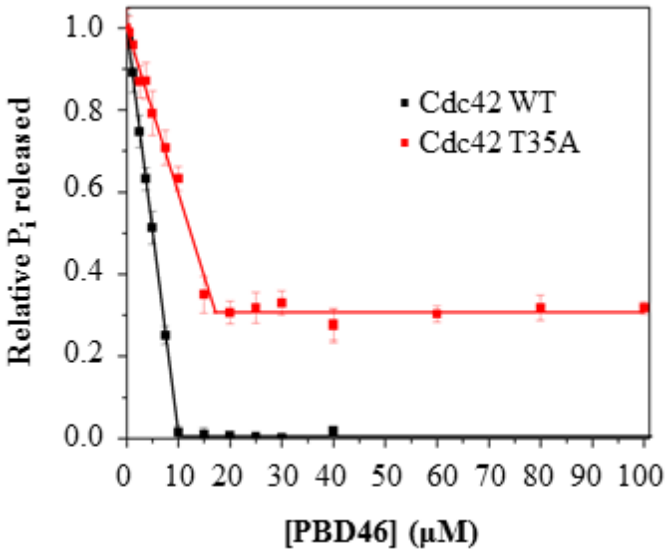

Figure 9. PBD46 concentration dependent GTP Hydrolysis. 10 μM Cdc42 (WT and T35A) (black and red, respectively) was assayed in the presence of increasing concentrations of PBD46. Saturation of Cdc42 WT occurs at 10 μM PBD46 ([Cdc42 WT]:[PBD46] = 1:1), at which point GTP hydrolysis is completely inhibited. Saturation of Cdc42 T35A occurs at 16 μM PBD46 ([Cdc42 WT]:[PBD46] = 1:1.6). T35A hydrolysis is only inhibited ~70% compared to 100% inhibition of WT hydrolysis at PBD46 saturation.

A time-dependent GTP hydrolysis assay of 10 μM Cdc42 (WT and T35A) in the absence and presence of 30 μM PBD46

was used to calculate and compare GTP hydrolysis rates according to the following equation:

$$P_i(t) = P_{i(max)} - \left(P_{i(max)} \text{ x } e^{-k_{obs}t}\right)$$

where $P_i(t)$ is the amount of inorganic phosphate released as a function of time (t), $P_{i(max)}$ is the maximum amount of inorganic phosphate released, and k_{obs} is the apparent first-order rate constant (**Figure 10**). Consistent with previous results [38], Cdc42 WT showed a high rate of GTP hydrolysis (95.5 ± 4.8 nmol P_i released) after 90 minutes in comparison to Cdc42 WT in the presence of PBD46 (0 nmol P_i released). As there was no hydrolysis, this supports previous observations that PBD46 inhibits hydrolysis of Cdc42 WT. Examination of the T35A mutation in the absence of PBD46 showed similar results to WT after 90 minutes (92.6 ± 5.4 nmol P_i released), translating to similar first-order rate constants (0.0868 ± 0.0044 min^{-1} and 0.0839 ± 0.0086 min^{-1}, respectively). Upon addition of PBD46, hydrolysis was partially restored for Cdc42 T35A (32.5 ± 4.3 nmol P_i released) with a slower first-order rate constant of 0.0459 ± 0.0047 min^{-1}. These results are summarized in **Table 2**.

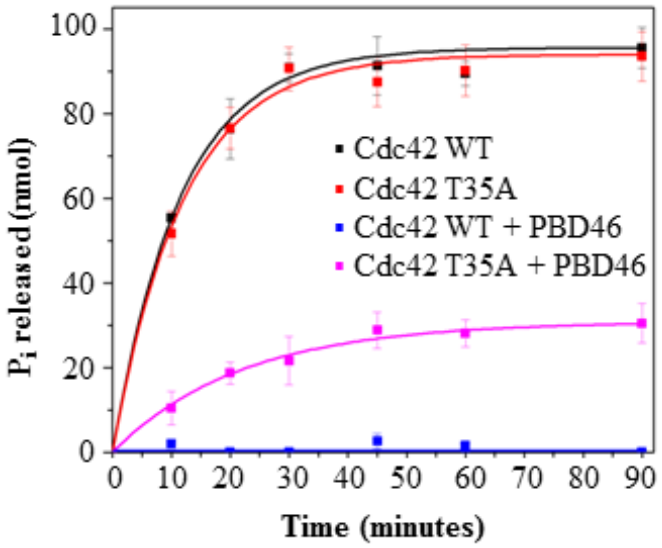

Figure 10. Time-dependent Cdc42 GTP Hydrolysis Assay. 10 μM Cdc42 (WT and T35A) was assayed in the absence and presence of 30μM PBD46 (1:3 [Cdc42]:[PBD46]. Cdc42 WT and T35A show comparable GTP hydrolysis. In the presence of PBD46, intrinsic GTP hydrolysis is completely inhibited for Cdc42 WT. Cdc42 T35A exhibits partial restoration of hydrolysis in the presence of PBD46.

	$P_{i\ max}$ (nmol)	K_{obs} (min^{-1})
Cdc42 WT	95.5 ± 4.8	0.0868 ± 0.0044
Cdc42 WT + PBD46	N/A	
Cdc42 T35A	92.6 ± 5.4	0.0839 ± 0.0086
Cdc42 T35A + PBD46	32.5 ± 4.3	0.0459 ± 0.0047

Table 2. $P_{i\ max}$ and K_{obs} for Cdc42 (WT and T35A) in the absence and presence of PBD46 determined via a time-dependent GTP hydrolysis

Although the T35A mutation does not appear to affect the intrinsic GTP hydrolysis rate for Cdc42 in comparison to WT, the partial restoration of GTP hydrolytic activity in the presence of PBD46 observed for the T35A mutation can be attributed to the weaker binding affinity between the GTPase and its effector. This exhibits a link between the conformational flexibility and effector binding; the more rigid switch I region of Cdc42 T35A binds more weakly to PBD46, partially restoring GTP hydrolysis.

Our results show that, as a result of this weaker binding, some of the intrinsic GTP hydrolysis is restored in the presence of the GTPase inhibitor PBD46. The different slopes of the linear decrease in P_i released at low PBD46 concentrations for Cdc42 WT and Cdc42 T35A (**Figure 9**) are evidence that K_d for PBD46 binding to Cdc42 T35A is lower than that observed for WT, which is approximately 20 nM [38]. The difference in K_{obs}, taken together with the difference in $P_{i\ max}$ observed for Cdc42 T35A in the presence of PBD46 compared to Cdc42 WT

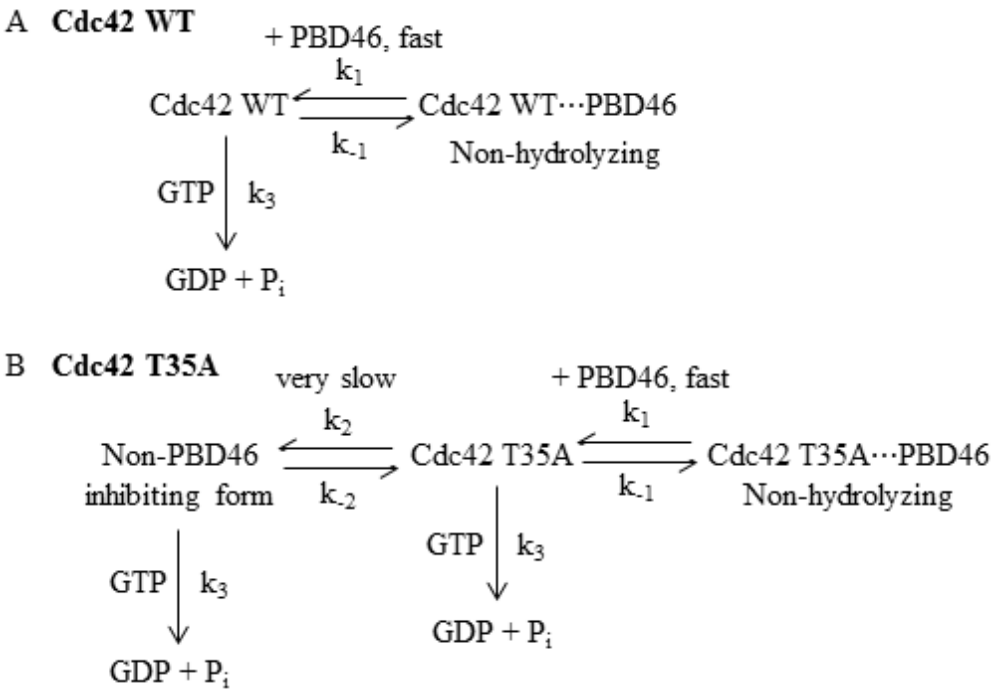

Figure 11. Proposed Cdc42 Kinetic Scheme. (A) Upon Cdc42 WT binding to PBD46, complete inhibition of GTP hydrolysis occurs as a result of tight binding. (B) Upon saturation of PBD46, Cdc42 T35A shows a reduced amount of hydrolysis compared to that in the absence of PBD46, but complete inhibition is not seen, implying that there may be two interconverting conformational states with different binding affinities to PBD46.

in the presence of PBD46, is telling of two conformations of Cdc42 T35A that have slow interconversion rates (**Figure 11B**), which is an idea that has been hypothesized for *Ras* T35A [33]. Although both conformations of Cdc42 T35A are capable of hydrolyzing GTP, one form has weakened or diminished binding to PBD46 which prevents PBD46 from completely inhibiting hydrolysis. The first order rate constants are the same for Cdc42 WT and T35A in the absence of PBD46, seen in **TABLE 2**, as a result of kinetics studies (**Figure 10**); this supports the proposed model of interconverting T35A conformational states that are both capable of exhibiting intrinsic GTP hydrolysis.

3.2 Characterization of the Interaction between Rheb and truncated Tuberous Sclerosis Complex 2 Constructs

The GAP domain of TSC2 is highly conserved across many species ranging from yeast to human [77, 78]. This GAP domain binds to Rheb *in vitro* and *in vivo*. Mutations in the GAP domain have been described as leading to the onset of the diseased state of tuberous sclerosis, due to the function of the GAP domain to increase intrinsic GTP hydrolysis activity of Rheb [46, 53-55, 68-70] (**Figure 2**). Neither the underlying mechanism by which TSC2 catalyzes GTP hydrolysis nor the details of the protein interaction are yet completely understood.

As a control, we confirmed binding between Rheb and TSC2-218 through an *in vitro* binding assay of GST-tagged TSC2-218 with Rheb. The concept lies in using the affinity tags to identify protein interactions. If any untagged protein appeared in the elution, it would show that the proteins were in complex. The specific GST-tag was exploited. One of multiple assays showed complex formation (**FIGURE 12**). In the elution peak, a band for

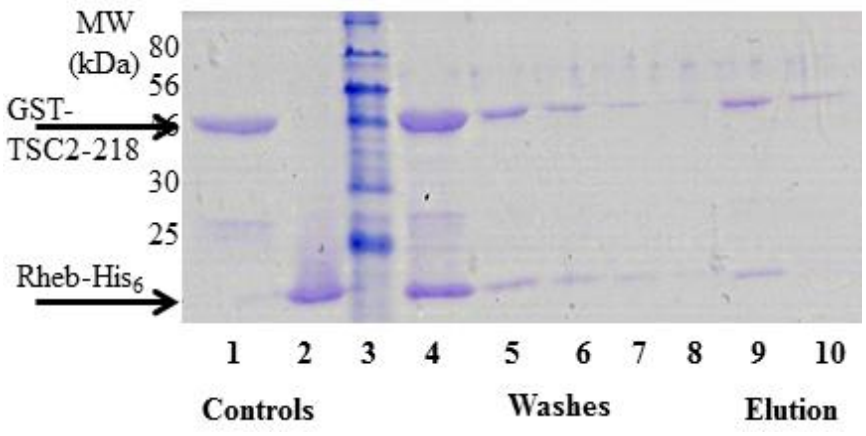

Figure 12. *In vitro* binding pull-down assay. Lanes 1 and 2 show the GST-TSC2-218 WT and Rheb controls, respectively. Lane 3 shows the molecular weight marker. Lane 4 shows the GST-TSC2-218-Rheb mixture before incubation. Lanes 5-8 show subsequent washes. Lanes 9 and 10 show subsequent elutions. In the final wash before elution (lane 8), there is little to no protein shown. In the first elution (lane 9), bands representative of both Rheb and GST-TSC2-218 appear. Because glutathione beads were used, the only way for Rheb to appear in the elution is if it were bound to GST-TSC2-218, which bound to the beads. This confirms complex formation.

GST-TSC2-218 (51 kDa) and a band for Rheb (21 kDa) appear. Rheb did not appear in the last wash before the elution; this leads to the conclusion that the only way Rheb could appear in the elution is if it was bound to GST-TSC2-218. Rheb alone does not bind to the glutathione sepharose. Size-exclusion chromatography, which separates protein systems based on size, was next applied. The large complex (72 kDa) would elute before the unbound GST-TSC2-218 and Rheb (51 kDa and 21 kDa, respectively) (**Figure 13A**).

It was necessary to use GST-tagged TSC2-218 in order to separate the complex from both unbound samples due to the resolution limits of the column. When the complex peak was run on SDS-PAGE, one band does not appear at the complex molecular weight (72 kDa), but rather a band appears representing each individual protein of the complex; the composition of the sample dye used for SDS-PAGE breaks the complex into its separate components. The approximately

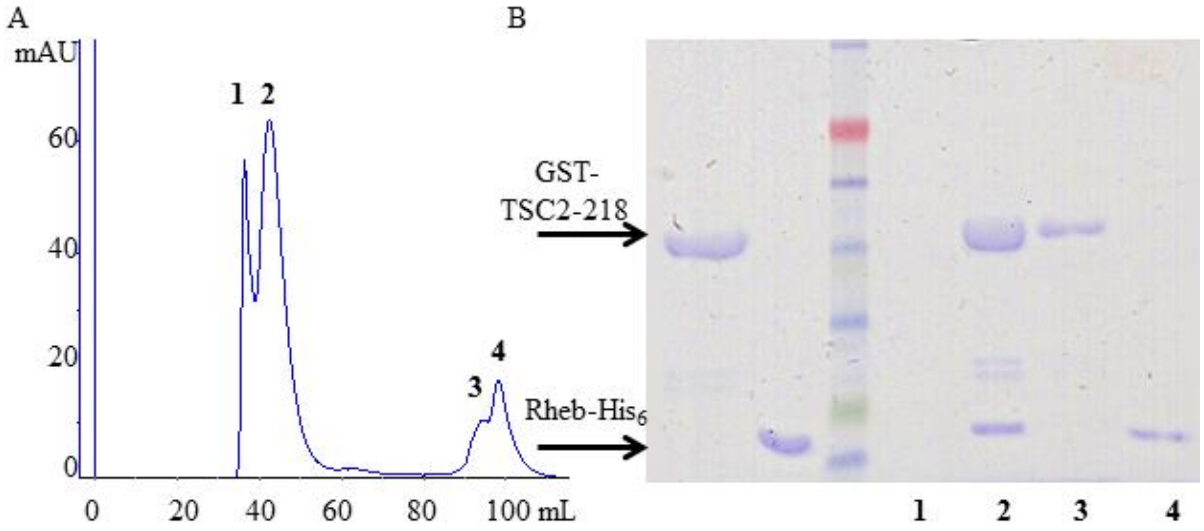

Figure 13. *In vitro* binding assay of equimolar GST-TSC2-218 WT and Rheb. (A) FPLC size exclusion chromatogram showing complex (peak 2), unbound GST-TSC2-218 (peak 3), and unbound Rheb (peak 4). (B) SDS-PAGE results following size exclusion chromatography. The first three lanes represent the control of GST-TSC2-218 WT and Rheb, respectively, followed by the molecular weight marker. Lane 3 contains the molecular weight marker. Lanes labeled 1-4 represent peaks 1-4 from the chromatogram showing the absence of protein, complex, unbound GST-TSC2-218, and unbound Rheb, respectively.

equal intensities of unbound GST-TSC2-218 and Rheb suggest that the binding is 1:1 as the assay was done with equimolar starting concentrations of the proteins (**Figure 13B**).

Once our controls had been established, a tuberous sclerosis associated single point mutation was designed. The K114A (K138A in full-length TSC2) substitution has been observed in tuberous sclerosis patients and so it was of interest to investigate what effects this point mutation had on the TSC2-218 – Rheb interaction and GAP function of TSC2-218 [79]. Other point mutations at this residue eliminated GAP activity [45]. Once expression and purification of TSC2-218 K114A were achieved, an *in vitro* binding assay with Rheb was done. The proteins were loaded onto a size-exclusion column as done for WT (page 14) (**Figure 14**). An elution peak for unbound GST-TSC2-218 WT as well as for Rheb was seen. However, unlike with wild-type TSC2-218, no complex formation was observed with TSC2-218 K114A (**FIGURE**

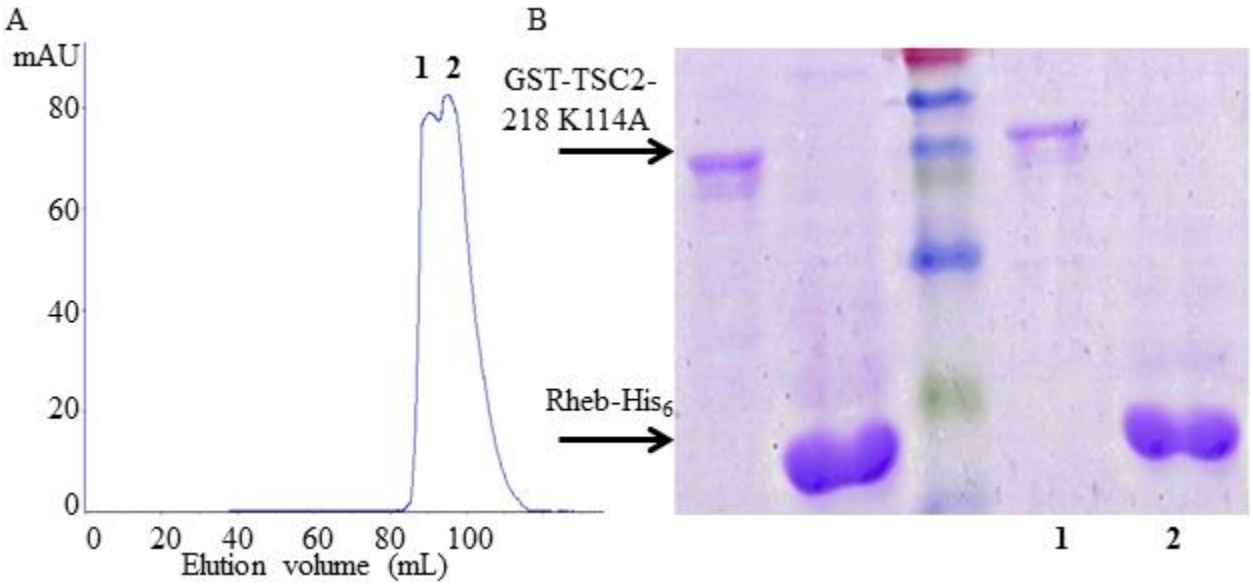

Figure 14. *In vitro* binding assay of equimolar GST-TSC2-218 K114A and Rheb. (A) FPLC size exclusion (S100) chromatogram showing unbound GST-TSC2-218 K114A (peak 1), unbound Rheb (peak 2), and lack of complex formation. (B) SDS-PAGE results following size exclusion chromatography. The first two lanes represent the control of GST-TSC2-218 K114A and Rheb, respectively, followed by the molecular weight marker. Lanes labeled 1 and 2 correspond to peaks 1 and 2 from the chromatogram showing unbound GST-TSC2-218 K114A and unbound Rheb, respectively. There is no complex formation.

14A), evidenced by the lack of peak at 45 mL elution. This preliminarily shows that TSC2-218 K114A does not interact with Rheb and, therefore, cannot act as a GAP to regulate cell signaling.

Circular dichroism (CD) and differential scanning calorimetry (DSC) were used to characterize the TSC2-218 mutant in comparison to the wild-type. TSC2-218 WT shows slight secondary structure, but a change in secondary structure is seen in TSC2-218 K114A (**Figure 15A**). The difference in secondary structure of the K114A mutant parallels a 5°C decrease in thermal stability as compared to WT (TSC2-218 unfolds at 60.6 ± 0.32°C and TSC2-218 K114A at 55.5 ± 0.42°C) (**Figure 16**). A CD comparison of TSC2-218 WT in the absence and presence of Rheb shows that upon binding to Rheb, there is a slight change in the secondary structural features of TSC2-218 WT (**Figure 15B)**, possibly supporting some form of an induced-fit model of binding. Conversely, there is no change evident in TSC2-218 K114A in the presence or absence of Rheb (**Figure 15C**). As changes in secondary structure were induced by the single-point mutation, a limited chymotrypsin digestion assay was used to monitor for any differences in cleavage patterns when exposed to chymotrypsin at an enzyme to protein ratio of 1:15. As **Figure 17** shows, different cleavage patterns were seen for WT and K114A, resulting in cleavage of 14% of TSC2-218 WT

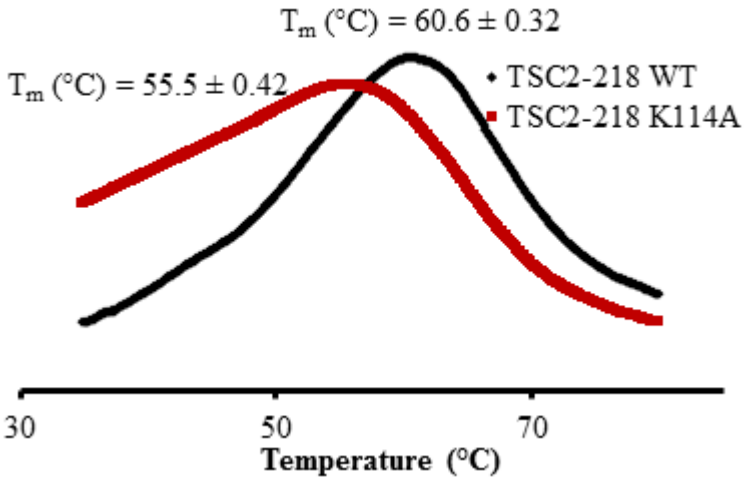

Figure 16. Differential Scanning Calorimetry. TSC2-218 WT exhibits a T_m of 60.6 ± 0.32°C. A 5°C decrease in thermal stability of TSC2-218 K114A is seen with a T_m of 55.5 ± 0.42°C.

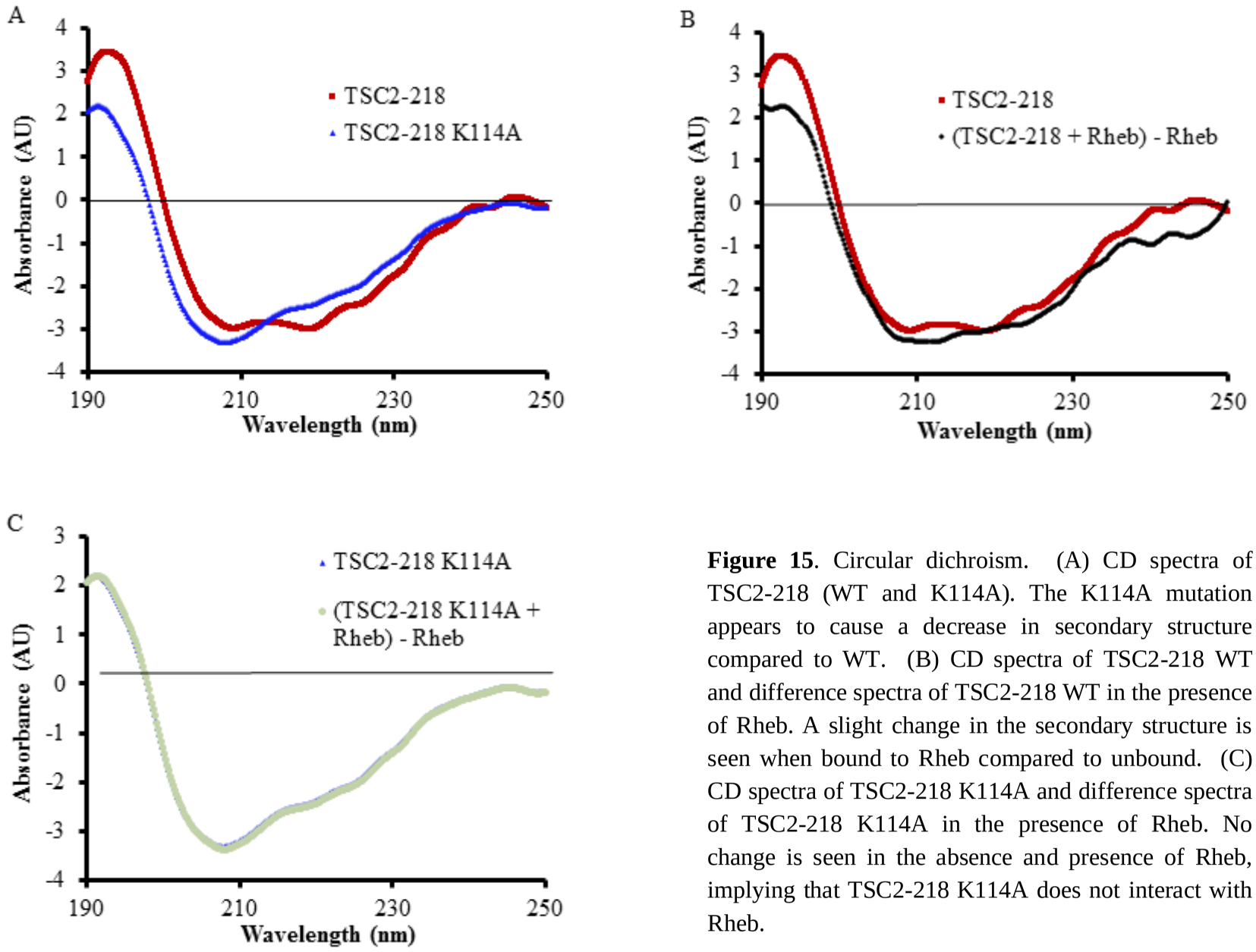

Figure 15. Circular dichroism. (A) CD spectra of TSC2-218 (WT and K114A). The K114A mutation appears to cause a decrease in secondary structure compared to WT. (B) CD spectra of TSC2-218 WT and difference spectra of TSC2-218 WT in the presence of Rheb. A slight change in the secondary structure is seen when bound to Rheb compared to unbound. (C) CD spectra of TSC2-218 K114A and difference spectra of TSC2-218 K114A in the presence of Rheb. No change is seen in the absence and presence of Rheb, implying that TSC2-218 K114A does not interact with Rheb.

and only 9.8% cleavage of TSC2-218 K114A after 180 minutes exposure to chymotrypsin activity. As chymotrypsin cleaves at the carboxylic side of aromatic amino acids, no change would be expected in cleavage patterns unless a conformational change was induced; some conformational change imparted by the K114A mutation leads to slight protection from enzymatic cleavage.

Rheb differs from other *Ras* proteins in that it has an intrinsically low rate of GTP hydrolysis and requires regulation to prevent overactivity; the activity of TSC2-218 WT as a GAP functions to regulate this activity by facilitating GTP hydrolysis [55]. In order to compare the TSC2-stimulated GAP activity of Rheb between TSC2-218 WT and K114A, we examined the GTP hydrolysis of Rheb alone and in the presence of TSC2-218 (**Figure 18)**. Consistent with previous results [45], Rheb showed essentially no intrinsic GTP hydrolysis (6.8997 ± 2.4703 nmol P_i released). After 120 minutes, Rheb in the presence of TSC2-218 WT released 61.7143 ± 1.3788 nmol P_i with a $T_{½}$ of 23.1 minutes compared to 6.8997 ± 2.4703 nmol P_i released in the absence of TSC2-218 WT (**Table 3)**. In the presence of TSC2-218 K114A, no

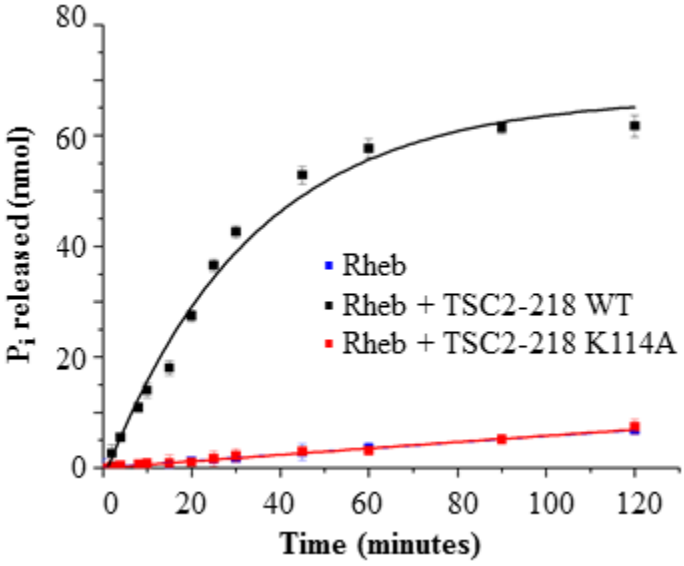

Figure 18. Time-dependent Rheb GTP Hydrolysis Assay. 10 μM Rheb was assayed in the absence and presence of 30μM TSC2-218 (WT and K114A) (1:3 [Rheb]:[TSC2-218]). In the absence of TSC2-218, Rheb shows very little intrinsic hydrolysis over time, displaying its characteristic "locked" GTP-bound state. Upon addition of TSC2-218 WT, GTP hydrolysis is facilitated. In the presence of TSC2-218 K114A, no increase in hydrolysis is seen in comparison to Rheb alone.

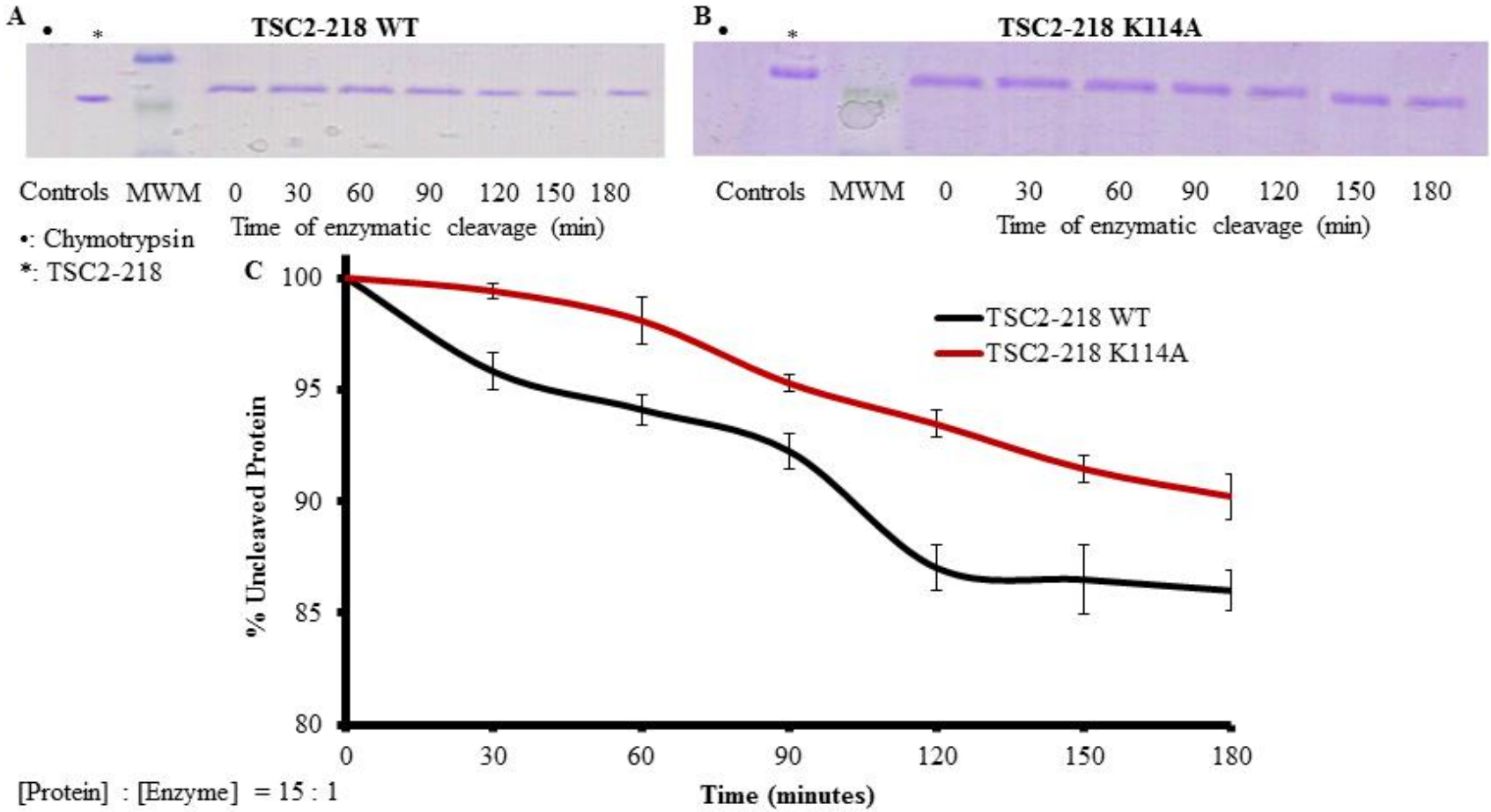

Figure 17. Limited Chymotrypsin Digestion. Representative SDS-PAGE of the products of digestion for TSC2-218 WT (A) and K114A (B). The gels show the chymotrypsin (•) and TSC2-218 (*) controls, the molecular weight marker, and the digestion products as a function of exposure time. (C) Graphical depiction of the percent of uncleaved TSC2-218 WT (black) and TSC2-218 K114A (red).

Sample	$T_{½}$	k
Rheb[A]	1029 min	6.7×10^{-4} min^{-1}
Rheb + TSC2-218 WT[A]	21.7 min	3.1×10^{-2} min^{-1}
Rheb + TSC2-218 WT[B]	23.1 min	$3.0 \times 10^{-2} \pm 0.003$ min^{-1}

Table 3. $T_{½}$ and rate constant for Rheb GTP Hydrolysis. Comparable values were obtained via the molybdate method used here ([B]) and NMR-based assay used by Marshall, et al ([A])

increase in GTP hydrolysis was evident (7.4167 ± 0.8124 nmol P_i released).

A concentration-dependent GTP hydrolysis assay of 10 µM Rheb in the presence of increasing concentrations of TSC2-218 (WT and K114A) was used to compare GTP hydrolysis according to the following equation:

$$P_i = \frac{P_{i(max)} \cdot [TSC2-218]^n}{K^n + [TSC2-218]^n}$$

where P_i is the amount of inorganic phosphate released, K is the apparent association constant, and n is the Hill coefficient, which gives an idea of cooperativity and may give information on the number of ligand binding sites

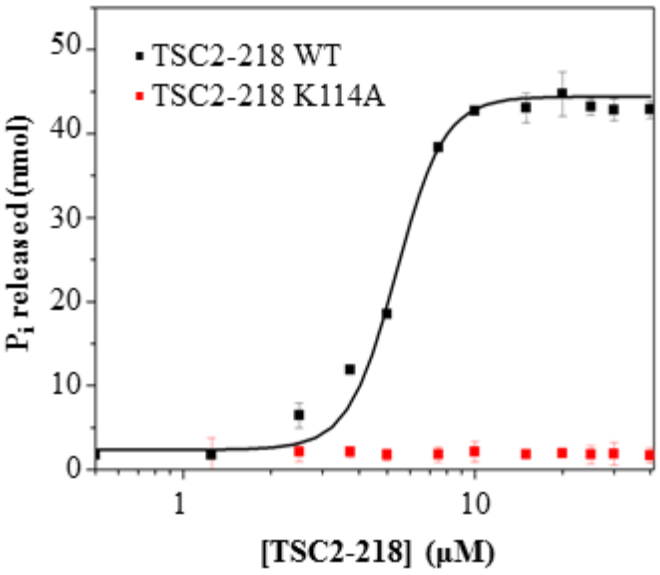

Figure 19. TSC2-218-concentration dependent GTP Hydrolysis Assay. 10 µM Rheb was assayed for 30 minutes in the presence of increasing concentrations of TSC2-218 (WT and K114A). The binding constant and Hill coefficient were calculated from the Rheb – TSC2-218 WT curve.

(**Figure 19**). The TSC2-218 WT – Rheb interaction released a maximal 44.4 ± 1.2 nmol P_i with a binding constant, K, of 5.4 ± 0.11 μM and a Hill coefficient of 5.3 ± 0.4. The positive Hill coefficient (5.3 ± 0.4) calculated from the sigmoidal kinetics studies (**Figure 19**) implies that there may be more than one binding domain for TSC2-218-Rheb binding.

2D HSQC NMR spectroscopy was used to determine if chemical shift changes occurred in ^{15}N-labeled Rheb in the absence and presence of TSC2-218. A 2D HSQC overlay of ^{15}N Rheb in the absence and presence of natural abundance TSC2-218 WT (**Figure 20A**) or TSC2-218 K114A (**Figure 20B**) did not show any discernible chemical shift changes as also shown by Marshall, et al.

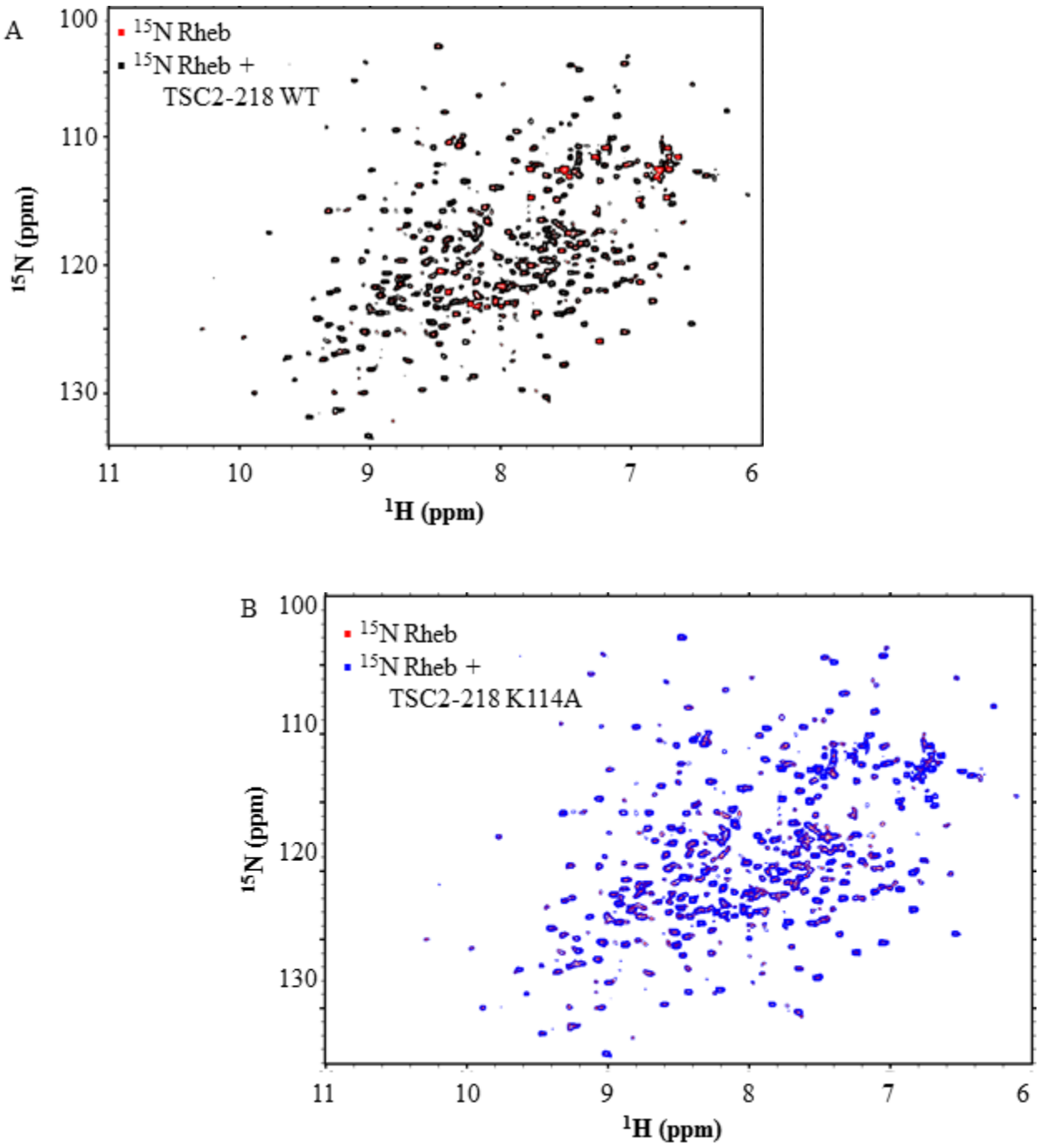

Figure 20. ^{15}N Rheb 2D HSQC NMR Spectroscopy. ^{15}N Rheb was run in the absence (red) and presence of (A) TSC2-218 WT (black) and (B) TSC2-218 K114A (blue). No chemical shift changes were evident in the presence of either TSC2-218 construct, although we know that binding occurs between Rheb and TSC2-218 WT. Spectra were obtained on Bruker Avance 700 MHz NMR using TopSpin and the data analyzed using Sparky software.

As there is no structural information to date on TSC2, it is of upmost importance to determine the structure to be able to fully characterize the TSC2-Rheb interaction. Tremendous efforts have also been unsuccessful in many other labs to obtain a 2D HSQC of TSC2-218 [87], perhaps due to the protein's tendency to aggregate at high concentrations needed for NMR. Protein prediction software predicted the structure of TSC2-218 to consist of ~25% α helix, ~25% β sheet, and ~50% random coil (**Figure 22**) [2]. Our attempts at obtaining a spectrum proved to be quite difficult. At lower TSC2-218 concentrations used for CD, DSC, etc., there were no problems with aggregation; at higher concentrations necessary for NMR, protein showed physical signs of aggregation in the NMR tubes, resulting in poor peak dispersion as evidenced in the spectra (**Figure 21**). Efforts to obtain spectra at 15°C in the presence of 10% glucose did not improve and reduce aggregation (not shown). We will continue to work with this protein and attempt change some aspects of the sample preparation in hopes to obtain an acceptable spectrum.

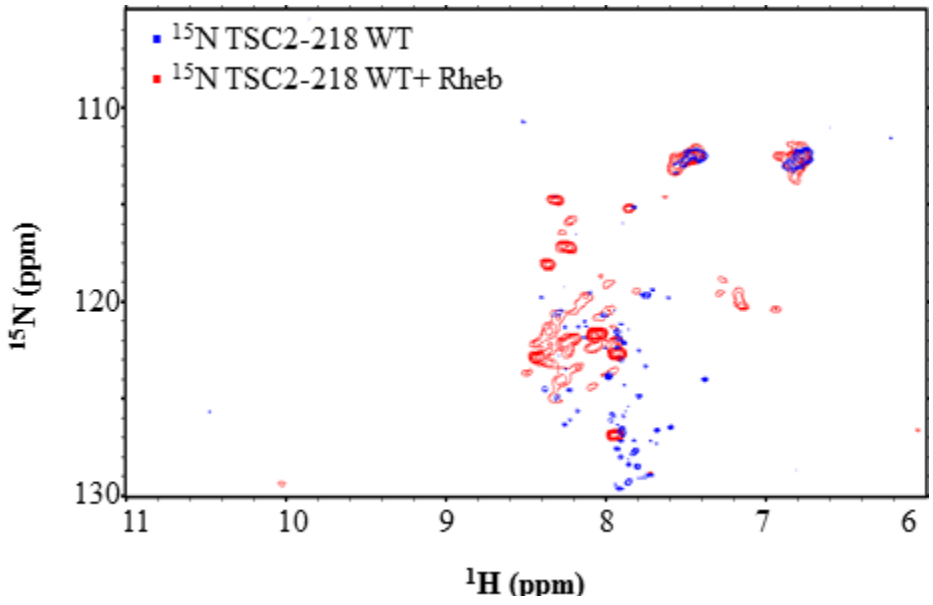

Figure 21. ^{15}N TSC2-218 WT 2D HSQC NMR Spectroscopy. ^{15}N TSC2-218 WT was run in the absence (blue) and presence (red) of Rheb. In both spectra, peaks characteristic of aggregation of evident. Spectra were obtained on Bruker Avance 700 MHz NMR using TopSpin and the data analyzed using Sparky Software.

4 Chapter 4: Conclusions and Future Directions

4.1 Intrinsic GTP Hydrolysis is observed for a Switch I Mutant of Cdc42 in the Presence of a Specific GTPase Inhibitor Peptide Derivative

Mutation of an invariant threonine residue in Cdc42, which causes a decrease in flexibility, does not affect the intrinsic GTP hydrolysis rate of Cdc42, but does alter the binding to an effector protein, PBD46. The disturbed binding leads to Cdc42 T35A GTP hydrolysis even in the presence of the GTPase inhibitor. As a result of our studies, we proposed the presence of multiple interconverting conformational states of Cdc42 T35A, one of which has a decreased affinity for PBD46.

Further characterization studies outlining the binding interface between PBD46 and Cdc42 T35A could give insight into the molecular details that lead to the less dynamic switch I region and highlight specific residues that contribute to weaker binding as well and make available a target for the design of ways to regulate protein interactions and, therefore, abnormal cell signaling. Fluorescence spectroscopy studies could be employed to study these two interconverting conformational states of Cdc42 T35A by calculating the K_D and NMR spectroscopy could be used to outline the Cdc42 T35A – PBD46 binding interface. If there was a way to restrict flexibility by binding small molecules, it may be possible to control oncogenic protein-protein interactions. Shown here, a decrease in flexibility in Cdc42 T35A leads to altered binding with an effector protein (PBD46). Since the idea of using small molecules to target oncogenic proteins was first conceptualized by Tavares, et al [80], recent studies have targeted *Ras* proteins with small molecules through the use of structure based drug design

(SBDD) [81]. More needs to be known on how this would affect the overall structure of the protein and if it would cause any unwanted/unexpected functional changes.

Unlike Cdc42 T35A which exhibits a slow exchange rate as a result of decreased flexibility, Cdc42 F28L is characterized by an increased exchange rate between GTP and GDP as a result of an increase in flexibility [85]. Ongoing studies using GTP may provide insight as to how the F28L mutation alters the affinity for the nucleotide. The structure-function relationship of this mutant needs to be further studied. Our lab is able to express and purify the mutant. Plans are underway to use DSC to compare the thermal stability of both the GTP- and GDP-bound forms of Cdc42 T35A with WT. Any differences might further explain why the fast-cycling occurs. GTP hydrolysis assays can also be employed to study the modification on hydrolysis in the absence and presence of PBD46. Pending the outcome of these results, NMR can be used to outline the binding interface and identify the changes in the structure-function relationship of Cdc42 T35A in comparison to Cdc42 WT.

4.2 Characterization of the Interaction between Rheb and truncated Tuberous Sclerosis Complex 2 Constructs

Rheb differs from other *Ras* proteins in that it has an intrinsically low rate of GTP hydrolysis and requires regulation to prevent overactivity; the activity of TSC2-218 WT as a GAP functions to regulate this activity, as shown in **Figure 18**. There is no structural information to date on TSC2 though protein prediction software predicted the structure of TSC2-218 to consist of ~25% α helix, ~25% β sheet, and ~50% random coil (**Figure 22**) [2]. It is of upmost importance to determine the structure to be able to fully characterize the TSC2-Rheb interaction. Although efforts in our lab as well as in many other labs to obtain a 2D HSQC of

TSC2-218 has proven to be quite difficult [87], we will continue to work with this protein and attempt to change some aspects of the sample preparation in hopes to obtain an acceptable spectrum. The TSC2 binding domain of TSC1 has recently been gifted by Wenqing Xu (University of Washington). Based on TSC1's stabilizing role when in complex in TSC2 [63, 64], pending successful transformation, growth and expression, TSC1 may prove to be necessary in complex with TSC2-218 in order to determine the structure of TSC2-218 WT. If this proves to be unmanageable, we may need to turn our efforts to X-ray crystallography in order to get a structure of TSC2-218 for comparison with and without Rheb.

Figure 22. Structure prediction of TSC2-218 WT using I-TASSER.

The disease-causing mutant TSC2-218 K114A was shown here to not function as a GAP for Rheb (**Figure 18**), allowing for Rheb to remain in a "locked" GTP-bound active state. The biophysical studies presented here lead to the conclusion that the single-point mutation causes secondary structure changes that result in an altered interaction with Rheb. Is the loss of binding to Rheb a result of a change in conformation that prevents access to the binding site or are the molecular details of the binding site altered? As we begin to understand the chemical and biological details of this protein interaction, we now have a platform on which to expand the studies of structure-function relationships of these proteins, with particular interest to mutations that alter structure and function.

Another mutant, the $Asn^{119} \rightarrow Lys^{119}$ mutant of TSC2-218 (equivalent to $Asn^{1643} \rightarrow Lys^{1643}$ in full-length TSC2), is a disease-causing mutation of what is thought to be the catalytic asparagine residue required for the asparagine thumb mechanism by which TSC2 increases GTPase activity of Rheb [45, 88]. The mutation removes an amide group and replaces it with a basic amine. Previous studies of other disease-associated point mutations of the proposed catalytic asparagine thumb have eliminated the GAP activity of TSC2 [45]. Pending successful mutation design and expression, we plan to further study and characterize TSC2-Rheb binding by studying the N119K mutation in the same manner as the K114A mutation.

In TSC2, exploration of another disease-causing mutation D1690 (D74 in TSC2-218), which lies in a region adjacent to the binding domain, did not inhibit GAP activity towards Rheb *in vitro* [45]. Unlike with many other mutants studied, it is not clear as to why this mutation is disease-causing *in vivo*. Is it possibly that this residue is, in part, responsible stabilizing Rheb in complex with TSC2? Further studies on this residue and its importance to TSC2 might reveal a new mechanism for oncogenic nature that has not been identified.

A mutant of Rheb in which the cysteine responsible for farnesylation is mutated to serine, thereby removing the free sulfur group, Rheb (C181S), shows a lower GTP level but still interacts with TSC2[46, 62]. Recent work has hypothesized that farnesylation is important for Rheb stimulation by GEF and that the GEF is responsible for the decreased ratio of GTP:GDP binding [50]. It would be beneficial to identify a Rheb GEF in order to develop ways to block or alter the interaction; without Rheb GEFs, Rheb may be more susceptible to be in the GDP-bound inactive state.

Much still remains unknown about the Rheb/TSC2 interaction, especially directed at TSC2. Although multiple studies have been done, there is still no sure answer as to whether TSC1 plays a role in TSC2-stimulated GTPase activity of Rheb. TSC1 has been shown to be required by several groups [53, 55, 62] while other groups have shown that it is not required [46, 50]. What function does the TSC1/TSC2 heterodimer display that is different from either TSC1 or TSC2 alone? It is possible that TSC1 is only required for stabilization of TSC2 [63], but it may play a more significant role than has been identified. Very recently, Tre2-Bub2-Cdc16 1 domain family, member 7 (TBC1D7) has been identified as a third core subunit of the TSC1/TSC2 complex and preliminary studies have shown that the complex formed (TSC-TBC) functions as a Rheb-GAP by sensing cellular growth conditions [89]. As new information, much more in depth research needs to be done to outline and understand completely the interaction and its mechanism.

4.3 CONCLUSIONS

Ras-like GTPases are of biological importance for their GTP hydrolysis mechanism; they are signal transduction proteins responsible for sending signals to the cell nucleus. Their role in cell signaling cascades will always be the target for studies as long as improper interactions occur *in vivo* that play a role in abnormal cell signaling activities.

The studies presented here are centered on understanding the relationship that lies between structure and function in *Ras*-related proteins. Most oncogenic *Ras* proteins are locked in a continuously active state, often facilitated by mutations that alter the intrinsic GTP-hydrolytic activity [90]. Structural changes imparted by something as small as a single point mutation can drastically alter the function of the protein. The threonine to alanine mutation in Cdc42 led to weaker binding and consequently partially restored the hydrolytic activity of Cdc42 in the

Cdc42-PBD46 interaction. As preliminarily seen in the Rheb-TSC2 interaction, the lysine to alanine point mutation (K114A) inhibited the interaction, possibly leading to overactivity of Rheb and prolonged cell signaling. Further exploration of these mutations, as well as the asparagine to lysine point mutation (N119K) and aspartic acid to alanine mutation (D74A) in TSC2-218 and the phenylalanine to leucine mutation (F28L) in Cdc42, are needed for characterization of the effects imparted by these mutations on the structure and function of these proteins and their interactions as part of a regulatory process.

A better understanding of the significance of changes on structure in *Ras* proteins is needed; it is necessary to provide a direct link between molecular aspects of interactions between proteins and begin to identify ways to regulate or alter aberrant cell signaling. Hopefully, this work can provide a foundation to promote the discovery of molecular features of *Ras* proteins that can aid in the modulation of the interactions that lead to diseased-states. In order to exploit any of these proteins as potential drug targets, much more needs to be understood concerning the protein-protein interactions, with a special interest in those interactions affected by mutations.

REFERENCES

1. Yu, Y., Li, S., Xu, X., Li, Y., Guan, K., Arnold, E., and Ding, J. (2005) Structural basis for the unique biological function of small GTPase RHEB, In *J Biol Chem*, pp 17093-17100, United States.

2. Zhang, Y. (2008) I-TASSER server for protein 3D structure prediction, *BMC Bioinformatics 9*, 40.

3. Chandrashekar, R., Salem, O., Krizova, H., McFeeters, R., and Adams, P. D. (2011) A switch I mutant of Cdc42 exhibits less conformational freedom, *Biochemistry 50*, 6196-6207.

4. Yamagata, K., Sanders, L. K., Kaufmann, W. E., Yee, W., Barnes, C. A., Nathans, D., and Worley, P. F. (1994) Rheb, a growth factor- and synaptic activity-regulated gene, encodes a novel Ras-related protein, *The Journal of Biological Chemistry 269*, 16333-16339.

5. Shilo, B. Z., and Weinberg, R. A. (1981) DNA sequences homologous to vertebrate oncogenes are conserved in Drosophila melanogaster, *Proc Natl Acad Sci U S A 78*, 6789-6792.

6. DeFeo, D., Gonda, M. A., Young, H. A., Chang, E. H., Lowy, D. R., Scolnick, E. M., and Ellis, R. W. (1981) Analysis of two divergent rat genomic clones homologous to the transforming gene of Harvey murine sarcoma virus, *Proc Natl Acad Sci U S A 78*, 3328-3332.

7. Ellis, R. W., Defeo, D., Shih, T. Y., Gonda, M. A., Young, H. A., Tsuchida, N., Lowy, D. R., and Scolnick, E. M. (1981) The p21 src genes of Harvey and Kirsten sarcoma viruses originate from divergent members of a family of normal vertebrate genes, *Nature 292*, 506-511.

8. Shih, T. Y., Weeks, M. O., Young, H. A., and Scholnick, E. M. (1979) Identification of a sarcoma virus-coded phosphoprotein in nonproducer cells transformed by Kirsten or Harvey murine sarcoma virus, *Virology 96*, 64-79.

9. Barbacid, M. (1987) ras GENES, *Ann Rev Biochem 56*, 779-827.

10. Vetter, I. R., and Wittinghofer, A. (2001) The guanine nucleotide-binding switch in three dimensions, In *Science*, pp 1299-1304, United States.

11. McCormick, F., Clark, B. F., la Cour, T. F., Kjeldgaard, M., Norskov-Lauritsen, L., and Nyborg, J. (1985) A model for the tertiary structure of p21, the product of the ras oncogene, *Science 230*, 78-82.

12. Hall, B. E., Yang, S. S., Boriack-Sjodin, P. A., Kuriyan, J., and Bar-Sagi, D. (2001) Structure-based mutagenesis reveals distinct functions for Ras switch 1 and switch 2 in Sos-catalyzed guanine nucleotide exchange, In *J Biol Chem*, pp 27629-27637, United States.

13. Fasano, O., Crechet, J. B., De Vendittis, E., Zahn, R., Feger, G., Vitelli, A., and Parmeggiani, A. (1988) Yeast mutants temperature-sensitive for growth after random mutagenesis of the chromosomal RAS2 gene and deletion of the RAS1 gene, *EMBO J 7*, 3375-3383.

14. Mistou, M. Y., Jacquet, E., Poullet, P., Rensland, H., Gideon, P., Schlichting, I., Wittinghofer, A., and Parmeggiani, A. (1992) Mutations of Ha-ras p21 that define important regions for the molecular mechanism of the SDC25 C-domain, a guanine nucleotide dissociation stimulator, *EMBO J 11*, 2391-2397.

15. Verrotti, A. C., Crechet, J. B., Di Blasi, F., Seidita, G., Mirisola, M. G., Kavounis, C., Nastopoulos, V., Burderi, E., De Vendittis, E., Parmeggiani, A., and et al. (1992) RAS residues that are distant from the GDP binding site play a critical role in dissociation factor-stimulated release of GDP, *EMBO J 11*, 2855-2862.

16. Jurnak, F. (1985) Structure of the GDP domain of EF-Tu and location of the amino acids homologous to ras oncogene proteins, *Science 230*, 32-36.

17. Reinstein, J., Schlichting, I., Frech, M., Goody, R. S., and Wittinghofer, A. (1991) p21 with a phenylalanine 28----leucine mutation reacts normally with the GTPase activating protein GAP but nevertheless has transforming properties, *J Biol Chem 266*, 17700-17706.

18. Saraste, M., Sibbald, P. R., and Wittinghofer, A. (1990) The P-loop--a common motif in ATP- and GTP-binding proteins, *Trends Biochem Sci 15*, 430-434.

19. Valencia, A., Chardin, P., Wittinghofer, A., and Sander, C. (1991) The ras protein family: evolutionary tree and role of conserved amino acids, *Biochemistry 30*, 4637-4648.

20. Urano, J., Tabancay, A. P., Yang, W., and Tamanoi, F. (2000) The Saccharomyces cerevisiae Rheb G-protein is involved in regulating canavanine resistance and arginine uptake, *The Journal of Biological Chemistry 275*, 11198-11206.

21. Yamagata, K., Sanders, L. K., Kaufmann, W. E., Yee, W., Barnes, C. A., Nathans, D., and Worley, P. F. (1994) rheb, a growth factor- and synaptic activity-regulated gene, encodes a novel Ras-related protein, *J Biol Chem 269*, 16333-16339.

22. Seeburg, P. H., Colby, W. W., Capon, D. J., Goeddel, D. V., and Levinson, A. D. (1984) Biological properties of human c-Ha-ras1 genes mutated at codon 12, *Nature 312*, 71-75.

23. Chipperfield, R. G., Jones, S. S., Lo, K. M., and Weinberg, R. A. (1985) Activation of Ha-ras p21 by substitution, deletion, and insertion mutations, *Mol Cell Biol 5*, 1809-1813.

24. Santos, E., Reddy, E. P., Pulciani, S., Feldmann, R. J., and Barbacid, M. (1983) Spontaneous activation of a human proto-oncogene, *Proc Natl Acad Sci U S A 80*, 4679-4683.

25. Pincus, M. R., van Renswoude, J., Harford, J. B., Chang, E. H., Carty, R. P., and Klausner, R. D. (1983) Prediction of the three-dimensional structure of the transforming

region of the EJ/T24 human bladder oncogene product and its normal cellular homologue, *Proc Natl Acad Sci U S A 80*, 5253-5257.

26. Pincus, M. R., and Brandt-Rauf, P. W. (1985) Structural effects of substitutions on the p21 proteins, *Proc Natl Acad Sci U S A 82*, 3596-3600.

27. Fasano, O., Aldrich, T., Tamanoi, F., Taparowsky, E., Furth, M., and Wigler, M. (1984) Analysis of the transforming potential of the human H-ras gene by random mutagenesis, *Proc Natl Acad Sci U S A 81*, 4008-4012.

28. Li, G., and Zhang, X. C. (2004) GTP Hydrolysis Mechanism of Ras-like GTPases, *Journal of Molecular Biology 340*, 921-932.

29. Der, C. J., Krontiris, T. G., and Cooper, G. M. (1982) Transforming genes of human bladder and lung carcinoma cell lines are homologous to the ras genes of Harvey and Kirsten sarcoma viruses, *Proc Natl Acad Sci U S A 79*, 3637-3640.

30. Temeles, G. L., Gibbs, J. B., D'Alonzo, J. S., Sigal, I. S., and Scolnick, E. M. (1985) Yeast and mammalian ras proteins have conserved biochemical properties, *Nature 313*, 700-703.

31. Scheffzek, K., Ahmadian, M. R., Kabsch, W., Wiesmuller, L., Lautwein, A., Schmitz, F., and Wittinghofer, A. (1997) The Ras-RasGAP complex: structural basis for GTPase activation and its loss in oncogenic Ras mutants, *Science 277*, 333-338.

32. Freymann, D. M., Keenan, R. J., Stroud, R. M., and Walter, P. (1999) Functional changes in the structure of the SRP GTPase on binding GDP and Mg2+GDP, *Nat Struct Biol 6*, 793-801.

33. Spoerner, M., Herrmann, C., Vetter, I. R., Kalbitzer, H. R., and Wittinghofer, A. (2001) Dynamic properties of the Ras switch I region and its importance for binding to effectors, *Proc Natl Acad Sci U S A 98*, 4944-4949.

34. Li, G., and Zhang, X. C. (2004) GTP hydrolysis mechanism of Ras-like GTPases, In *J Mol Biol*, pp 921-932, England.

35. Maegley, K. A., Admiraal, S. J., and Herschlag, D. (1996) Ras-catalyzed hydrolysis of GTP: a new perspective from model studies, *Proc Natl Acad Sci U S A 93*, 8160-8166.

36. Leonard, D., Hart, M. J., Platko, J. V., Eva, A., Henzel, W., Evans, T., and Cerione, R. A. (1992) The identification and characterization of a GDP-dissociation inhibitor (GDI) for the CDC42Hs protein, *J Biol Chem 267*, 22860-22868.

37. Bos, J. L. (1989) ras oncogenes in human cancer: a review, *Cancer Res 49*, 4682-4689.

38. Guo, W., Sutcliffe, M. J., Cerione, R. A., and Oswald, R. E. (1998) Identification of the binding surface on Cdc42Hs for p21-activated kinase, In *Biochemistry*, pp 14030-14037, United States.

39. Nassar, N., Horn, G., Herrmann, C., Scherer, A., McCormick, F., and Wittinghofer, A. (1995) The 2.2 A crystal structure of the Ras-binding domain of the serine/threonine kinase c-Raf1 in complex with Rap1A and a GTP analogue, *Nature 375*, 554-560.

40. Gizachew, D., and Oswald, R. E. (2001) Concerted motion of a protein-peptide complex: backbone dynamics studies of an (15)N-labeled peptide derived from P(21)-activated kinase bound to Cdc42Hs.GMPPCP, In *Biochemistry*, pp 14368-14375, United States.

41. Gizachew, D., Guo, W., Chohan, K. K., Sutcliffe, M. J., and Oswald, R. E. (2000) Structure of the complex of Cdc42Hs with a peptide derived from P-21 activated kinase, In *Biochemistry*, pp 3963-3971, United States.

42. Feltham, J. L., Dotsch, V., Raza, S., Manor, D., Cerione, R. A., Sutcliffe, M. J., Wagner, G., and Oswald, R. E. (1997) Definition of the switch surface in the solution structure of Cdc42Hs, In *Biochemistry*, pp 8755-8766, United States.

43. Fiordalisi, J. J., Holly, S. P., Johnson, R. L., 2nd, Parise, L. V., and Cox, A. D. (2002) A distinct class of dominant negative Ras mutants: cytosolic GTP-bound Ras effector domain mutants that inhibit Ras signaling and transformation and enhance cell adhesion, In *J Biol Chem*, pp 10813-10823, United States.

44. Adams, P. D., and Oswald, R. E. (2007) NMR assignment of Cdc42T35A, an active Switch I mutant of Cdc42, *Biomol NMR Assign 1*, 225-227.

45. Marshall, C. B., Ho, J., Buerger, C., Plevin, M. J., Li, G. Y., Li, Z., Ikura, M., and Stambolic, V. (2009) Characterization of the intrinsic and TSC2-GAP-regulated GTPase activity of Rheb by real-time NMR, In *Sci Signal*, p ra3, United States.

46. Castro, A. F., Rebhun, J. F., Clark, G. J., and Quilliam, L. A. (2003) Rheb binds tuberous sclerosis complex 2 (TSC2) and promotes S6 kinase activation in a rapamycin- and farnesylation- dependent manner, *The Journal of Biological Chemistry 278*, 32493-32496.

47. Manning, B. D., and Cantley, L. C. (2003) Rheb fills a GAP between TSC and TOR, In *Trends Biochem Sci*, pp 573-576, England.

48. Tabancay, A. P., Jr., Gau, C. L., Machado, I. M., Uhlmann, E. J., Gutmann, D. H., Guo, L., and Tamanoi, F. (2003) Identification of dominant negative mutants of Rheb GTPase and their use to implicate the involvement of human Rheb in the activation of p70S6K, In *J Biol Chem*, pp 39921-39930, United States.

49. Aspuria, P.-J., and Tamanoi, F. (2004) The Rheb family of GTP-binding proteins, *Cellular Signaling 16*, 1105-1112.

50. Li, Y., Inoki, K., and Guan, K. L. (2004) Biochemical and functional characterizations of small GTPase Rheb and TSC2 GAP activity, In *Mol Cell Biol*, pp 7965-7975, United States.

51. Im, E., von Lintig, F. C., Chen, J., Zhuang, S., Qui, W., Chowdhury, S., Worley, P. F., Boss, G. R., and Pilz, R. B. (2002) Rheb is in a high activation state and inhibits B-Raf kinase in mammalian cells, *Oncogene 21*, 6356-6365.

52. Li, Y., Corradetti, M. N., Inoki, K., and Guan, K. L. (2004) TSC2: filling the GAP in the mTOR signaling pathway, In *Trends Biochem Sci*, pp 32-38, England.

53. Garami, A., Zwartkruis, F. J. T., Nobukuni, T., Joaquin, M., Roccio, M., Stocker, H., Kozma, S. C., Hafen, E., Bos, J. L., and Thomas, G. (2003) Insulin activation of Rheb, a mediator of mTOR/S6K/4E-BP signaling, is inhibited by TSC1 and 2, *Molecular Cell 11*, 1457-1466.

54. Tee, A. R., Manning, B. D., Roux, P. P., Cantley, L. C., and Blenis, J. (2003) Tuebrous sclerosis complex gene products, tuberin and hamartin, control mTOR signaling by acting as a GTPase-activating protein complex toward Rheb, *Current Biology 13*, 1259-1268.

55. Zhang, Y., Gao, X., Saucedo, L. J., Ru, B., Edgar, B. A., and Pan, D. (2003) Rheb is a direct target of the tuberous sclerosis tumour suppressor proteins, In *Nat Cell Biol*, pp 578-581, England.

56. van Slegtenhorst, M., de Hoogt, R., Hermans, C., Nellist, M., Janssen, B., Verheof, S., Lindhout, D., van den Ouweland, A., Halley, D., Young, J., Burley, M., Jeremiah, S., Woodward, K., Nahmias, J., Fox, M., Ekong, R., Osborne, J., Wolfe, J., Povey, S., Snell, R. G., Cheadle, J. P., Jones, A. C., Tachataki, M., Ravine, D., Sampson, J. R., Reeve, M. P., Richardson, P., Wilmer, F., Munro, C., Hawkins, T. L., Sepp, T., Ali, J. B. M., Ward, S., Green, A. J., Yates, J. R. W., Kwiatkoswka, J., Henske, E. P., Short, M. P., Hains, J. H., Jozwiak, S., and Kwiatkowski, D. J. (1997) Identifiaction of the Tuberous Sclerosis gene TSC1 on chromosome 9q34, *Science 277*, 805-808.

57. Huang, J., and Manning, B. D. (2008) The TSC1-TSC2 complex: a molecular switchboard controlling cell growth, In *Biochem J*, pp 179-190, England.

58. (1993) Identification and characterization of the tuberous sclerosis gene on chromosome 16, *Cell 75*, 1305-1315.

59. Maheshwar, M. M., Cheadle, J. P., Jones, A. C., Myring, J., Fryer, A. E., Harris, P. C., and Sampson, J. R. (1997) The GAP-related domain of tuberin, the product of the TSC2 gene, is a target for missense mutations in tuberous sclerosis, *Human Molecular Genetics 6*, 1991-1996.

60. Finlay, G. A., Malhowski, A. J., Liu, Y., Fanburg, B. L., Kwiatkowski, D. J., and Toksoz, D. (2007) Selective inhibition of growth of tuberous sclerosis complex 2 null cells by atorvastatin is associated with impaired Rheb and Rho GTPase function and reduced mTOR/S6 kinase activity, In *Cancer Res*, pp 9878-9886, United States.

61. Inoki, K., Li, Y., Xu, T., and Guan, K. L. (2003) Rheb GTPase is a direct target of TSC2 GAP activity and regulates mTOR signaling, In *Genes Dev*, pp 1829-1834, United States.

62. Tee, A. R., Manning, B. D., Roux, P. P., Cantley, L. C., and Blenis, J. (2003) Tuberous sclerosis complex gene products, Tuberin and Hamartin, control mTOR signaling by acting as a GTPase-activating protein complex toward Rheb, In *Curr Biol*, pp 1259-1268, England.

63. Benvenuto, G., Li, S., Brown, S. J., Braverman, R., Vass, W. C., Cheadle, J. P., Halley, D. J., Sampson, J. R., Wienecke, R., and DeClue, J. E. (2000) The tuberous sclerosis-1 (TSC1) gene product hamartin suppresses cell growth and augments the expression of the TSC2 product tuberin by inhibiting its ubiquitination, *Oncogene 19*, 6306-6316.

64. Chong-Kopera, H., Inoki, K., Li, Y., Zhu, T., Garcia-Gonzalo, F. R., Rosa, J. L., and Guan, K. L. (2006) TSC1 stabilizes TSC2 by inhibiting the interaction between TSC2 and the HERC1 ubiquitin ligase, In *J Biol Chem*, pp 8313-8316, United States.

65. Li, Y., Inoki, K., and Guan, K.-L. (2004) Biochemical and functional characterizations of small GTPase Rheb and TSC2 GAP activity, *Molecular and Cellular Biology 24*, 7965-7975.

66. Yu, Y., Li, S., Xu, X., Li, Y., Guan, K., Arnold, E., and Ding, J. (2005) Structural basis for the unique biological function of small GTPASE Rheb, *The Journal of Biological Chemistry 280*, 17093-17100.

67. Daumke, O., Weyand, M., Chakrabarti, P. P., Vetter, I. R., and Wittinghofer, A. (2004) The GTPase-activating protein Rap1GAP uses a catalytic asparagine, *Nature 429*, 197-201.

68. Wienecke, R., Konig, A., and DeClue, J. E. (1995) Identification of tuberin, the tuberous sclerosis-2 product. Tuberin possesses specific Rap1GAP activity, *J Biol Chem 270*, 16409-16414.

69. Xiao, G. H., Shoarinejad, F., Jin, F., Golemis, E. A., and Yeung, R. S. (1997) The tuberous sclerosis 2 gene product, tuberin, functions as a Rab5 GTPase activating protein (GAP) in modulating endocytosis, *J Biol Chem 272*, 6097-6100.

70. Marshall, C. B., Ho, J., Buerger, C., Plevin, M. J., Li, G.-Y., Li, Z., Ikura, M., and Stambolic, V. (2009) Characterization of the Intrinsic and TSC2-GAP-Regulated GTPase Activity of Rheb by Real-Time NMR, *Science Signaling 2*, ra3.

71. Marshall, C. B., Ho, J., Buerger, C., Plevin, M. J., Li, G.-Y., Li, Z., Ikura, M., and Stambolic, V. (2009) Characterizatoin of the intrinsic and TSC2-GAP-regulated GTPase activity of Rheb by real-time NMR, *Science Signaling 2*, 1-11, ra13.

72. Sambrook, J., and Russell, D. Q. (2001) Appendices, In *Molecular Cloning: A Laboratory Manual*, Cold Spring Harbor Laboratory Press, Cold Spring Harbor, New York.

73. J., S. B. (1988) Methods of Molecular Biology, pp 57-69, Humana Press, New Jersey.

74. Spackman, D. H., Stein, W. H., and Moore, S. (1960) The disulfide bonds of ribonuclease, *J Biol Chem 235*, 648-659.

75. Chifflet, S., Torriglia, A., Chiesa, R., and Tolosa, S. (1988) A method for the determination of inorganic phosphate in the presence of labile organic phosphate and high concentrations of protein: application to Lens ATPases, *Analytical Biochemistry 168*, 1-4.

76. Gonzalez-Romo, P., Sanchez-Nieto, S., and Gavilanes-Ruiz, M. (1992) A modified colorimetric method for the determination of orthophsophate in the presence of high ATP concentrations, *Analytical Biochemistry 200*, 235-238.

77. Maheshwar, M. M., Sandford, R., Nellist, M., Cheadle, J. P., Sgotto, B., Vaudin, M., and Sampson, J. R. (1996) Comparative analysis and genomic structure of the tuberous sclerosis 2 (TSC2) gene in human and pufferfish, *Hum Mol Genet 5*, 562.

78. Matsumoto, S., Bandyopadhyay, A., Kwiatkowski, D. J., Maitra, U., and Matsumoto, T. (2002) Role of the Tsc1-Tsc2 complex in signaling and transport across the cell membrane in the fission yeast Schizosaccharomyces pombe, *Genetics 161*, 1053-1063.

79. Au, K. S., Williams, A. T., Roach, E. S., Batchelor, L., Sparagana, S. P., Delgado, M. R., Wheless, J. W., Baumgartner, J. E., Roa, B. B., Wilson, C. M., Smith-Knuppel, T. K., Cheung, M. Y., Whittemore, V. H., King, T. M., and Northrup, H. (2007) Genotype/phenotype correlation in 325 individuals referred for a diagnosis of tuberous sclerosis complex in the United States, *Genet Med 9*, 88-100.

80. Taveras, A. G., Remiszewski, S. W., Doll, R. J., Cesarz, D., Huang, E. C., Kirschmeier, P., Pramanik, B. N., Snow, M. E., Wang, Y. S., del Rosario, J. D., Vibulbhan, B., Bauer, B. B., Brown, J. E., Carr, D., Catino, J., Evans, C. A., Girijavallabhan, V., Heimark, L., James, L., Liberles, S., Nash, C., Perkins, L., Senior, M. M., Tsarbopoulos, A., Webber, S. E., and et al. (1997) Ras oncoprotein inhibitors: the discovery of potent, ras nucleotide exchange inhibitors and the structural determination of a drug-protein complex, *Bioorg Med Chem 5*, 125-133.

81. Shima, F., Yoshikawa, Y., Ye, M., Araki, M., Matsumoto, S., Liao, J., Hu, L., Sugimoto, T., Ijiri, Y., Takeda, A., Nishiyama, Y., Sato, C., Muraoka, S., Tamura, A., Osoda, T., Tsuda, K., Miyakawa, T., Fukunishi, H., Shimada, J., Kumasaka, T., Yamamoto, M., and Kataoka, T. (2013) In silico discovery of small-molecule Ras inhibitors that display antitumor activity by blocking the Ras-effector interaction, *Proc Natl Acad Sci U S A 110*, 8182-8187.

82. de Vos, A. M., Tong, L., Milburn, M. V., Matias, P. M., Jancarik, J., Noguchi, S., Nishimura, S., Miura, K., Ohtsuka, E., and Kim, S. H. (1988) Three-dimensional structure of an oncogene protein: catalytic domain of human c-H-ras p21, *Science 239*, 888-893.

83. Pai, E. F., Kabsch, W., Krengel, U., Holmes, K. C., John, J., and Wittinghofer, A. (1989) Structure of the guanine-nucleotide-binding domain of the Ha-ras oncogene product p21 in the triphosphate conformation, *Nature 341*, 209-214.

84. Schlichting, I., John, J., Frech, M., Chardin, P., Wittinghofer, A., Zimmermann, H., and Rosch, P. (1990) Proton NMR studies of transforming and nontransforming H-ras p21 mutants, *Biochemistry 29*, 504-511.

85. Lin, R., Bagrodia, S., Cerione, R., and Manor, D. (1997) A novel Cdc42Hs mutant induces cellular transformation, In *Curr Biol*, pp 794-797, England.

86. Adams, P. D., and Oswald, R. E. (2006) Solution structure of an oncogenic mutant of Cdc42Hs, *Biochemistry 45*, 2577-2583.

87. Sun, W., Zhu, Y. J., Wang, Z., Zhong, Q., Gao, F., Lou, J., Gong, W., and Xu, W. (2013) Crystal structure of the yeast TSC1 core domain and implications for tuberous sclerosis pathological mutations, *Nat Commun 4*, 2135.

88. Maheshwar, M. M., Cheadle, J. P., Jones, A. C., Myring, J., Fryer, A. E., Harris, P. C., and Sampson, J. R. (1997) The GAP-related domain of tuberin, the product of the TSC2 gene, is a target for missense mutations in tuberous sclerosis, In *Hum Mol Genet*, pp 1991-1996, England.

89. Dibble, C. C., Elis, W., Menon, S., Qin, W., Klekota, J., Asara, J. M., Finan, P. M., Kwiatkowski, D. J., Murphy, L. O., and Manning, B. D. (2012) TBC1D7 Is a Third Subunit of the TSC1-TSC2 Complex Upstream of mTORC1, In *Mol Cell*, pp 535-546, 2012 Elsevier Inc, United States.

90. Ramirez de Molina, A., Rodriguez-Gonzalez, A., and Lacal, J. C. (2004) From Ras signalling to ChoK inhibitors: a further advance in anticancer drug design, In *Cancer Lett*, pp 137-148, Ireland.